POLITECNICO DI TORINO

Master of Science

in Mechanical Engineering

Master's Degree Thesis

Design of Torque Vectoring system for Formula SAE electric vehicle

Supervisors:

Prof. Alessandro Vigliani

Prof. Francisco Javier Paez

Candidate:

Andrea Fricano

UPM ETSII

University Institute of Automobile Research (INSIA)

October 2019

To my beloved family

and friends that have supported me all over years

A special thanks to my uncle Michi who surely looks proudly at me from up there

This is for you

Abstract

This thesis work has been carried out in Madrid at the university institute of automobile research (INSIA) linked to the UPM ETSII (Universidad Politécnica de Madrid, Escuela Técnica Superior de Ingenieros Industriales) as a part of the Erasmus+ programme. The supervisor at the research department was the professor Javier Francisco Paez.

With the evolution of technologies new active safety systems have been developed to guarantee a safer and more stable use of commercial vehicles. Torque Vectoring (TV) is an active control system that substitutes the need of a mechanical differential and it's widely used in racing and commercial electric vehicles.

This thesis has the objective to design a Torque Vectoring controller for a Formula SAE racing car that is equipped with 4 in-wheel electric motors. This control system, also known as dynamic control of traction, can improve the cornering performance of the vehicle by properly allocating the torque among the four independent electric motors.

Yaw rate is the main parameter used to define the stability behaviour of the vehicle; a physical model of the car is built up to generate a proper reference value of yaw rate. To design the controller first it's presented the generic vehicle model and then followed by the 2 DOF linear model of the car. The Torque Vectoring control system designed takes also into account the limits of adherence of wheels and the motor curve saturation.

The designed control system, built in Matlab Simulink, is implemented to the professional automotive control software CarSim and its performance is analysed in various manoeuvres. The results of all the simulations then are evaluated, and the effectiveness of the controller is determined.

Contents

List of tables

List of figures

Nomenclature

a	Distance between centre of gravity and front axle
a_x	Longitudinal acceleration
a_y	Lateral acceleration
A	Boolean variable for front left wheel
B	Boolean variable for front right wheel
C	Boolean variable for rear left wheel
D	Boolean variable for rear right wheel
α	Tire slip angle
α_f	Front tire slip angle
α_r	Rear tire slip angle
b	Distance between centre of gravity and rear axle
β	Side slip angle of the vehicle
$\dot{\beta}$	Side slip angle rate of the vehicle
$C_{\alpha f}$	Equivalent cornering stiffness of the front axle
$\widetilde{C_{\alpha_f}}$	Cornering stiffness of front tire
$C_{\alpha r}$	Equivalent cornering stiffness of the rear axle
$\widetilde{C_{\alpha_r}}$	Cornering stiffness of rear tire
δ	Steering angle
δ_f	Equivalent front steering angle
δ_{fL}	Front left wheel steering angle
δ_{fR}	Front right wheel steering angle
$\Delta F_{z_{lat}}$	Lateral transfer load
$\Delta F_{z_{long}}$	Longitudinal transfer load
$\Delta\dot{\psi}$	Yaw rate error
F_{yf}	Cornering force of front axle
F_{yr}	Cornering force of rear axle
F_{z_e}	Vertical load on wheels external to the curve

F_{zf}	Vertical load on front axle
F_{z_i}	Vertical load on wheels internal to the curve
F_{zfL}	Vertical load on front left wheel
F_{zfR}	Vertical load on front right wheel
F_{zrL}	Vertical load on rear left wheel
F_{zrR}	Vertical load on rear right wheel
g	Gravity acceleration
G_r	Epicyclical gear ratio
h_{CG}	Vertical height of centre of gravity
I_z	Inertia moment along z-axis of the car
κ_{acc}	Slip ratio in acceleration
κ_{dec}	Slip ratio in deceleration
$\kappa_{\lim}$	Limit slip ratio corresponding to the maximum longitudinal adherence coefficient
K_u	Understeer gradient
m_{CG}	Mass of the vehicle rigid body
M_z	Yaw moment required along z-axis
M_{zf}	Yaw moment required along z-axis in front axle
M_{zr}	Yaw moment required along z-axis in rear axle
R_{turn}	Curvature radius
S_{a_y}	Slope of the curve $\Delta\tau\ vs\ \Delta\dot{\psi}$ for lateral acceleration different from zero
S_r	Steer ratio
S_{V_x}	Slope of the curve $\Delta\tau\ vs\ \Delta\dot{\psi}$ for zero lateral acceleration
t_f	Front track of the vehicle
T	Torque
T_0	Stall torque of the motor
T_r	Throttle
T_{wheel}	Wheel torque
$T_{wheel_{MAX}}$	Maximum wheel torque

T_{max}	Maximum torque
T_{tot}	Total torque required
u	Longitudinal velocity of the vehicle
v	Lateral velocity of the vehicle
$\dot{v}$	Lateral velocity rate of the vehicle
v_{wheel_x}	Longitudinal velocity of the wheel
v_{wheel_y}	Lateral velocity of the wheel
V_x	Longitudinal speed of the vehicle
ψ	Yaw angle
$\dot{\psi}$	Yaw rate
$\dot{\psi}_{des}$	Yaw rate desired
$\dot{\psi}_{max}$	Yaw rate limit
$\dot{\psi}_{real}$	Real yaw rate
$\dot{\psi}_{ref}$	Yaw rate reference
$\ddot{\psi}$	Yaw rate variation
ω_{motor}	Spin rate of a motor
Ω_{wheel}	Spin rate of wheel
Ω_{ideal}	Ideal spin rate of wheel in pure rolling

Glossary

ABS: Anti-lock Braking System

ESP: Electronic Stability Program

TV: Torque Vectoring

SAE: Society of Automotive Engineers

FSAE: Formula SAE

UPM: Universidad Politécnica de Madrid

ETSII: Escuela Técnica Superior de Ingenieros Industriales

RPM: Revolutions per minute

CG: Centre of Gravity

SUV: Sport Utility Vehicle

ECU: Engine Control Unit

ODE: Ordinary Differential Equation

DLC: Double Lane Change

RMSD: Root Mean Square Deviation

NRMSD: Normalized Root Mean Square Deviation

DOF: Degree Of Freedom

Chapter 1: Introduction

This thesis work has been carried out in Madrid at the university institute of automobile research (INSIA) linked to the UPM ETSII (Universidad Politécnica de Madrid, Escuela Técnica Superior de Ingenieros Industriales). The work has been carried on during the period February/July 2019 during my participation at the Erasmus+ programme.

Electric vehicles have spread year after year with the continuous development of the automotive industry. Them, compared to vehicles with combustion engines, guarantee better efficiency and respect for the environment, since they do not exhaust polluting gases.

With the birth of the electric vehicles segment, new technological solutions have been proposed year after year to improve their efficiency and manoeuvrability.

The first electric vehicles used an electric motor positioned between the driving wheels through a mechanical differential. Now in an electric vehicle one or more motor are normally used; there are advantages and disadvantages in using more motors. There are electric vehicles in the market that use 1, 2 or 4 electric motors.

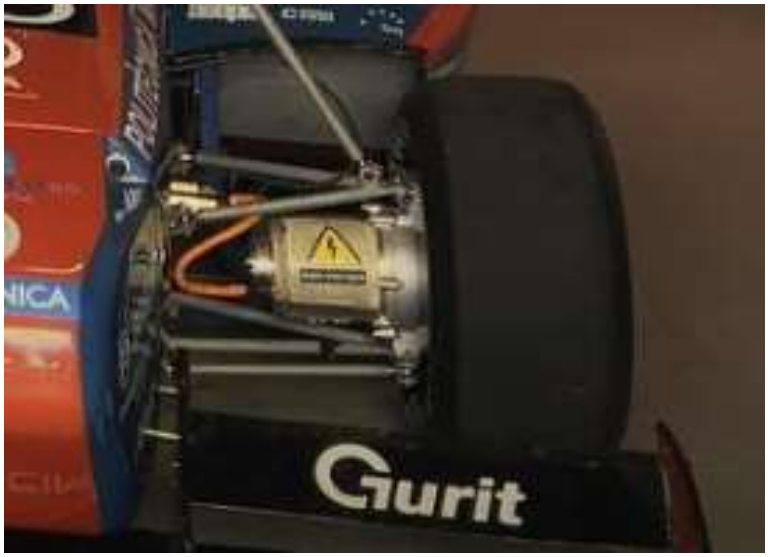

Figure 1: Hub Motor of a Formula SAE racing car

The motor configuration that permits the best condition of manoeuvrability of the vehicle is the one with 4 electric motors. The 4 motors can be mounted inside the body in white of the vehicle or in the hub; this last motor configuration is also known as in-wheel motors or hub motors, where the motors are connected to the wheels through a mechanical reducer consisting of a planetary gearbox.

This new solution introduces remarkable advantages: better controllability of the vehicle being able to control independently the 4 hub motors; however, it has also some disadvantages: difficulty of installation of the motors inside the wheel hub and mainly the increase of the unsprung mass of the vehicle. This last one is a main problem, since it changes the dynamic behaviour of the vehicle due to the different weight distribution that is now more concentrated in the wheels with respect to the case of motors mounted inside the body in white of the vehicle.

The selected vehicle to be studied is equipped with 4 in-wheel motors.

The use of electronic systems to control the stability of the vehicle has increased over the years to ensure safety while driving and nowadays different control systems are present in all commercial vehicles present on the market; two of these are ABS and ESP.

In this thesis work a control system called Torque Vectoring has been studied and developed. This system, called also dynamic control of traction, has been elaborated in the last years and it was initially used only for racing purposes. Nowadays, instead, it's also present in some expensive commercial vehicles.

Torque vectoring can improve the cornering performance of vehicles, and significantly in an all-wheel-drive vehicle being able to vary independently the torque to the four motors.

By properly allocate the torque to be assigned to each of the 4 electric motors, through this control system, it is possible to improve the response and the cornering dynamic performance of the vehicle.

The use of this control system can significantly improve the response of the car to a precise steering input guaranteeing a higher value of lateral acceleration and yaw rate for the same value of steering input; this leads to a better cornering performance of the vehicle.

Thanks to these features this control system is used for all the electric vehicles in the Formula SAE student competition to improve their overall performance, specifically in lateral dynamics. This thesis is based on the development of a TV control system for the electric vehicle built by UPM ETSII of Madrid participating at the international student competition Formula SAE.

1.1 Formula SAE Team and Car

Formula SAE is an international racing car competition between engineering university all over the world. Students work in team to develop a challenging racing car that must be able to compete in static and dynamic events. The static events consider design, manufacturing and cost; the dynamic events consider the performance of the car that is evaluated in a series of dynamic tests.

The team is made up of students from the university UPM ETSII of Madrid. The university has been developing in this academic year 2018/2019 a racing vehicle called UPM 03E that is the third version of their FSAE electric vehicle. The vehicle is represented in figure 2.

Figure 2: UPM 03E racing car

The UPM 03E vehicle is equipped with 4 electric motors; these servomotors are supplied by the company AMK. In figure 3 it's represented the data sheet of the servomotors used. Each motor has a maximum torque of 21 $N * m$ and RPM range 0 to 18000; they are connected to their corresponding wheel through a planetary gear with fixed ratio 13,176:1.

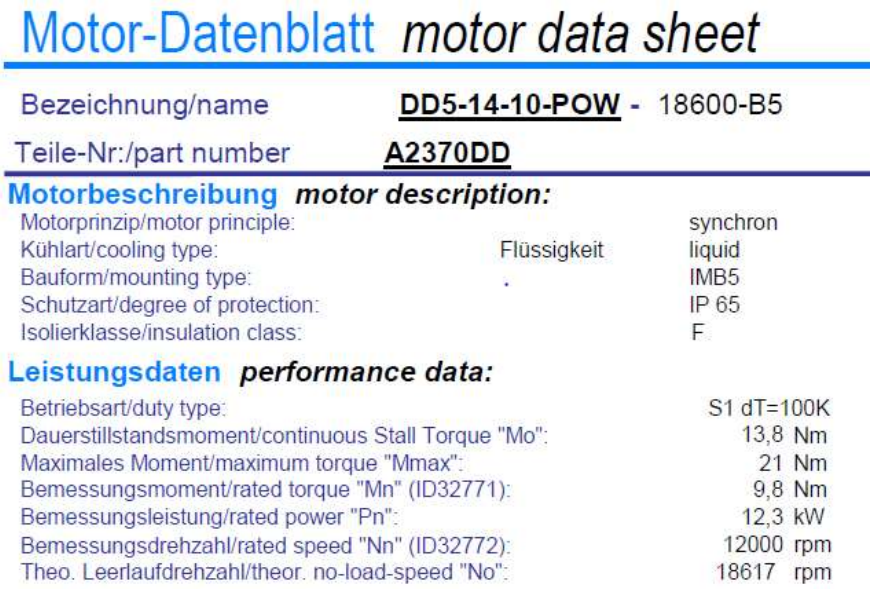

Motor-Datenblatt *motor data sheet*

Bezeichnung/name	**DD5-14-10-POW** - 18600-B5	
Teile-Nr:/part number	**A2370DD**	

Motorbeschreibung ***motor description:***

Motorprinzip/motor principle:		synchron
Kühlart/cooling type:	Flüssigkeit	liquid
Bauform/mounting type:	.	IMB5
Schutzart/degree of protection:		IP 65
Isolierklasse/insulation class:		F

Leistungsdaten ***performance data:***

Betriebsart/duty type:	S1 dT=100K
Dauerstillstandsmoment/continuous Stall Torque "Mo":	13,8 Nm
Maximales Moment/maximum torque "Mmax":	21 Nm
Bemessungsmoment/rated torque "Mn" (ID32771):	9,8 Nm
Bemessungsleistung/rated power "Pn":	12,3 kW
Bemessungsdrehzahl/rated speed "Nn" (ID32772):	12000 rpm
Theo. Leerlaufdrehzahl/theor. no-load-speed "No":	18617 rpm

Figure 3: AMK motor data sheet [1]

The vehicle can thus guarantee a total maximum torque to wheels equal to 1108 $N * m$.

All the main parameters of the car will be analysed and presented in chapter 2.

1.2 Objectives

The aim of this work is to improve the overall racing performance of the car UPM 03E represented in figure 2; to meet this objective a torque vectoring control system is designed to properly allocate the torque among the four wheels of the vehicle.

The fact that the vehicle is equipped with 4 engines makes the use of torque vectoring fundamental and it's expected a better result than in using it in vehicles that own one or two motors.

By correctly allocating the torque to the wheels it is possible to improve the dynamic response of the vehicle for a given steering input, guaranteeing a big gain in the cornering dynamic behaviour of the vehicle.

1.3 Thesis outline

Chapter 2 introduces the vehicle dynamics and the model used to describe its behaviour. First all the main dynamic variables of the vehicle and tires are introduced; the linear tire model used to define the yaw rate reference is then defined. The main parameters of the car are described.

In chapter 3 the TV controller is developed step by step and all its different blocks are presented with their internal structure; the sensors used to track the needed state variables of the car are detailed.

In chapter 4 simulations are carried on; they are conducted by using Matlab Simulink in a co-simulated environment with the vehicle performance software CarSim. Simulations are carried on in different driving conditions comparing the use of the controller with the case of torque equally allocated among the wheels. In this way the benefits brought by using this TV control system are assessed and the effectiveness is evaluated through its advantages.

Chapter 2: Vehicle Dynamic

Vehicle dynamic means applying the dynamic principles to a vehicle in order to study its motion with time. The knowledge of the main features of vehicle dynamics is important to understand the behaviour of a vehicle during its driving conditions.

The main dynamic characteristics on a vehicle are:

- Longitudinal dynamic
- Lateral dynamic
- Tire dynamic
- Suspensions dynamic
- Aerodynamic effects

Each of them must be carefully applied to properly understand the overall dynamic behaviour of a car and the dynamic principles must be applied to study all these characteristics.

Longitudinal dynamics explains the behaviour of the vehicle during acceleration and braking; instead, lateral dynamics define the directional and cornering behaviour of the car.

Tire dynamic is fundamental to properly understand the contact in between wheel and ground; the forces exchanged in this contact are the ones that allows the vehicle to move.

At the end, suspension dynamics and aerodynamic effects have a big influence on the vehicle dynamic since they influence in a big amount the transfer load among wheels and the aerodynamic load that permits the vehicle to accelerate at higher g's.

These dynamic features of the vehicles can not be considered alone, since they influence each other by changing the behaviour of the vehicle and they have to be all considered to avoid errors.

The vehicle model with all the cartesian reference axes is presented in the following paragraph.

2.1 Vehicle Model

A vehicle has three main cartesian reference frames to be considered:

- Inertial cartesian frame
- Vehicle cartesian frame
- Tire cartesian frame

In the following figure (figure 4) it is represented in blue the inertial cartesian frame and in yellow the rigid body cartesian frame (of the vehicle CG).

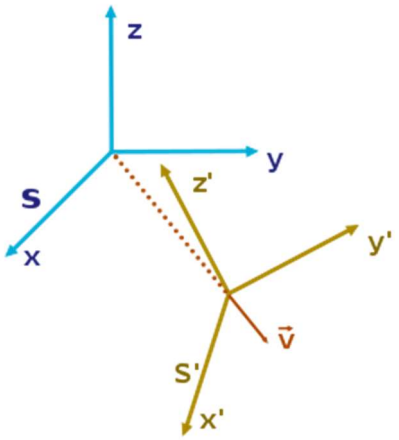

Figure 4: Inertial and rigid body cartesian frame of the vehicle [2]

The inertial frame (blue) is fixed in a point of the space; the vehicle reference frame (yellow) is centred in the vehicle CG and it moves with it during time.

In figure 5 it's represented the vehicle CG reference frame with the main rotations and angles that characterize a vehicle.

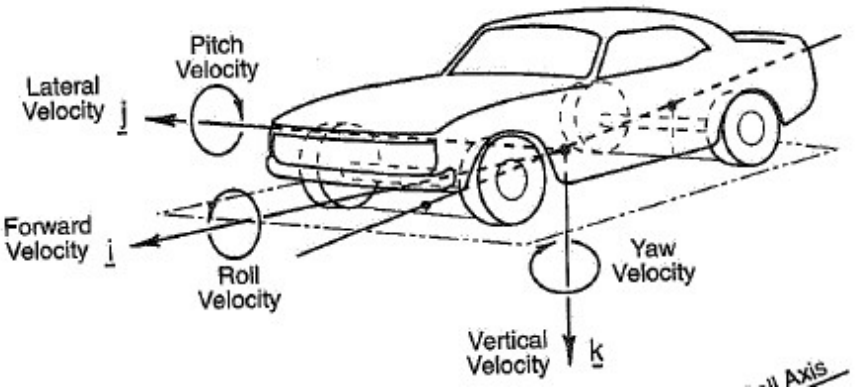

Figure 5: Vehicle reference frame with main rotations [3]

A vehicle can rotate around three orthogonal axes centred on its centre of gravity.

These axes are the following: longitudinal (X), lateral (Y) and vertical (Z). The three rotations about these axes must be properly considered in car dynamics; these rotations are known as: roll, pitch and yaw motions.

These motions are explained in the following paragraphs.

2.1.1 Roll

The roll motion is represented in figure 6 for a generic car vehicle. Roll is the rotation of the car around the longitudinal axis (X) and it affects the way how the weight of the vehicle is laterally distributed.

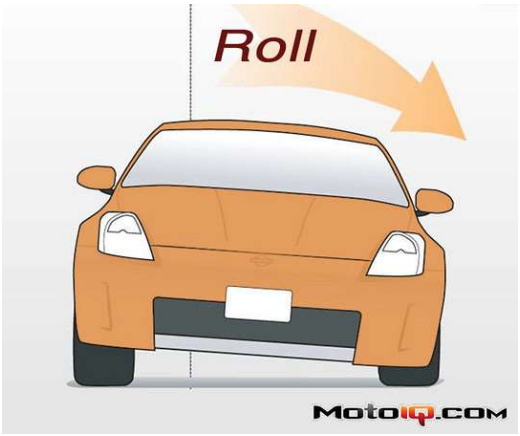

Figure 6: Roll rotation of a vehicle [4]

While taking a turn there's a load transfer from the internal to the external wheels as it possible to see in the figure 7.

The rolling moment can influence both positively and negatively the cornering behaviour of a vehicle.

Roll motion can be controlled properly with the use of anti-roll bars; this element helps to reduce the roll motion of the vehicle during turns. The Formula SAE vehicle UPM 03E is equipped with an anti-roll bar in the front axle. The roll stiffness of the vehicle influences the lateral load transfer on the front axle. The presence of an anti-roll bar in the front axle changes the dynamic cornering behaviour of the vehicle influencing also the understeer behaviour of the vehicle, resulting in a vehicle with a more accentuated understeer character. The influence of the presence of the anti-roll bar will be considered in the car model implemented in the simulation software CarSim. In this part of the work, the lateral load transfer is considered to be influenced only by the lateral acceleration of the vehicle.

During a turn the load on the wheels is laterally transferred due to the centrifugal acceleration:

$$a_y = \frac{V_x^2}{R_{turn}} \tag{1}$$

In figure 7 it is represented the lateral load transferred to the external wheels. The amount of load transferred from internal to external wheels:

$$\Delta F_{Z_{lat}} = \frac{m_{CG} * a_y * h_{CG}}{t_f} \tag{2}$$

The total load in the internal and external wheels are thus:

$$F_{z_i} = \frac{m_{CG} * g}{2} - \Delta F_{Z_{lat}} = \frac{m_{CG} * g}{2} - \frac{m_{CG} * a_y * h_{CG}}{t_f} \tag{3}$$

$$F_{z_e} = \frac{m_{CG} * g}{2} + \Delta F_{Z_{lat}} = \frac{m_{CG} * g}{2} + \frac{m_{CG} * a_y * h_{CG}}{t_f} \tag{4}$$

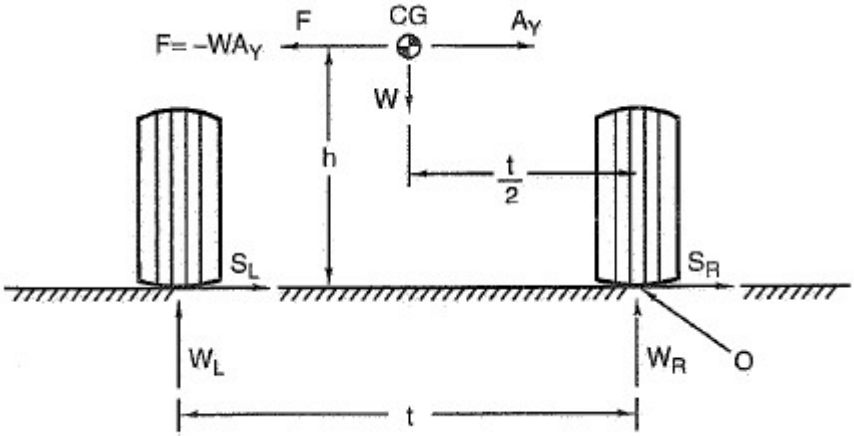

Figure 7: Lateral load transfer due to lateral acceleration during a turn [3]

2.1.2 Pitch

Pitch is the rotation of a car around the lateral axis (Y) and it affects the way how the weight is longitudinally distributed.

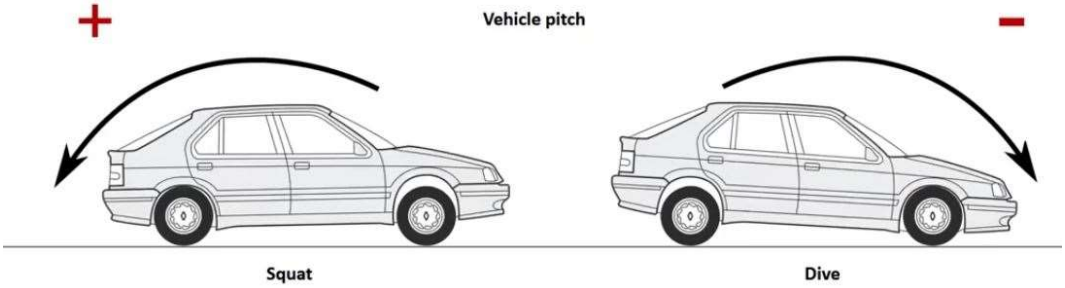

Figure 8: Pitch rotation of a vehicle [4]

When a vehicle is accelerating its weight is transferred to the rear wheels giving more adherence to them and the vehicle bend backward (squat rotation); this is a big advantage for rear drive and all-wheel drive vehicles, thus it can guarantee a powerful acceleration. Instead, when a car is braking its weight is transferred to the front wheels and it leans forward (dive rotation).

During acceleration and braking load is longitudinally transferred due to the longitudinal acceleration.

$$a_x = \frac{d}{dt} V_x \tag{5}$$

In figure 9 it is represented how the load is longitudinally transferred.

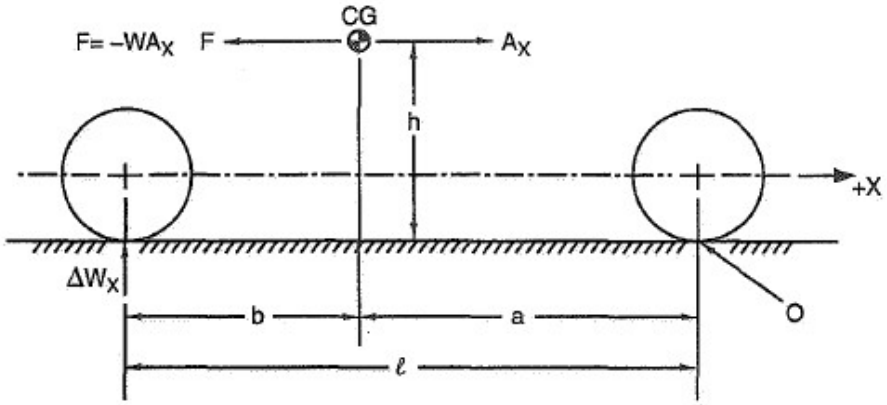

Figure 9: Longitudinal load transfer due to longitudinal acceleration [3]

The amount of longitudinal transfer load from front to rear axle during acceleration is:

$$\Delta F_{Z_{long}} = \frac{m_{CG} * a_x * h_{CG}}{a + b} \tag{6}$$

If the vehicle is braking, the longitudinal acceleration changes sign (becoming negative) and weight is transferred from the rear to the front axle.

Since normally the position of the CG is not symmetric with respect to the two axles, a different amount of load is distributed to rear and front axle even when the vehicle is still.

The amount of vertical load onto the two axles considering the geometrical construction of the vehicle and the longitudinal load transfer due to an acceleration manoeuvre is thus:

$$F_{zf} = \frac{b}{a + b} * m_{CG} * g - \Delta F_{Z_{long}} = \frac{b}{a + b} * m_{CG} * g - \frac{m_{CG} * a_x * h_{CG}}{a + b} \tag{7}$$

$$F_{zr} = \frac{b}{a + b} * m_{CG} * g + \Delta F_{Z_{long}} = \frac{b}{a + b} * m_{CG} * g + \frac{m_{CG} * a_x * h_{CG}}{a + b} \tag{8}$$

2.1.3 Load on wheels considering transfer loads due to accelerations

By considering the amount of load transferred in the equations (2) and (6) due to the corresponding lateral and longitudinal acceleration the amount of load in each wheel can be re-written as:

$$F_{zfL} = \frac{\frac{b}{a+b} * m_{CG} * g - \frac{m_{CG} * a_x * h_{CG}}{a+b}}{2} - \frac{m_{CG} * a_y * h_{CG}}{2 * t_f} \quad (9)$$

$$F_{zfR} = \frac{\frac{b}{a+b} * m_{CG} * g - \frac{m_{CG} * a_x * h_{CG}}{a+b}}{2} + \frac{m_{CG} * a_y * h_{CG}}{2 * t_f} \quad (10)$$

$$F_{zrL} = \frac{\frac{b}{a+b} * m_{CG} * g + \frac{m_{CG} * a_x * h_{CG}}{a+b}}{2} - \frac{m_{CG} * a_y * h_{CG}}{2 * t_f} \quad (11)$$

$$F_{zrR} = \frac{\frac{b}{a+b} * m_{CG} * g + \frac{m_{CG} * a_x * h_{CG}}{a+b}}{2} + \frac{m_{CG} * a_y * h_{CG}}{2 * t_f} \quad (12)$$

These are the vertical loads on the four wheels of the vehicle.

It must be added that in the formulas previously written (equations 9, 10, 11 and 12) the vertical loads considered on the wheels are influenced only by the geometry of the vehicle and the longitudinal and lateral acceleration. These formulas are profoundly influenced by aerodynamic effects and by the presence of an anti-roll bar in the front axle of the vehicle. These two effects will be considered when implementing the control system in the co-simulating environment with the CarSim software and its model which takes into account the effects of aerodynamic loads and the different roll stiffness of the two axles of the vehicle.

2.1.4 Yaw

Yaw rotation about z-axis is represented in figure 10.

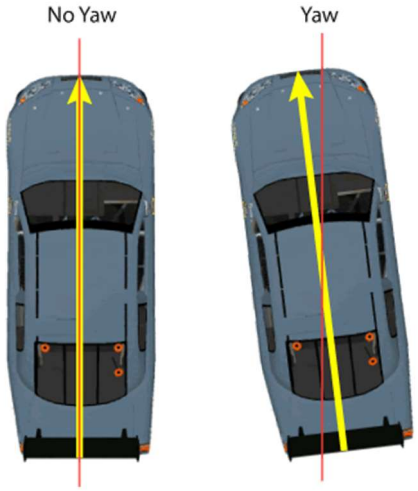

Figure 10: Yaw rotation of a vehicle [4]

Yaw (also known as heading angle) describes the rotation of a car around the vertical axis (Z). The yaw angle is in between the longitudinal axis of the vehicle (X) and the vehicle's velocity vector. Yaw is an angle and it is normally measured in rad or deg; it will be indicated by the letter ψ.

The yaw rate is the rate of change in time of it and it's normally measured in rad/s or deg/s. It will be indicated by $\dot{\psi}$.

When a car goes straight, normally, there's no angle between the x-axis and velocity direction so the yaw angle is null. When, instead, a vehicle is performing a turn yaw angle and rate are generally not null.

When a vehicle performs a curve there's an imbalanced moment that causes the vehicle to rotate about the vertical axis and this rotation is called yaw motion.

The higher is the value of yaw the quicker a car turns when entering in a curve; but a value too high of yaw or yaw rate can cause instability when driving the car.

Another important variable to describe is the yaw moment (measured normally in N*m), indicated with M_z, which is the moment about the z-axis (known also as yaw axis).

By properly controlling the yaw rate of the vehicle it's possible to provide perfect cornering ability also with low grip roads.

The control system that will be presented in chapter 3 is based on yaw rate tracking reference.

2.1.5 Side-slip angle of the vehicle

In vehicle dynamics slip angle is the angle between the direction in which a body points and the direction in which it moves; this angle is indicated in figure 11 with β.

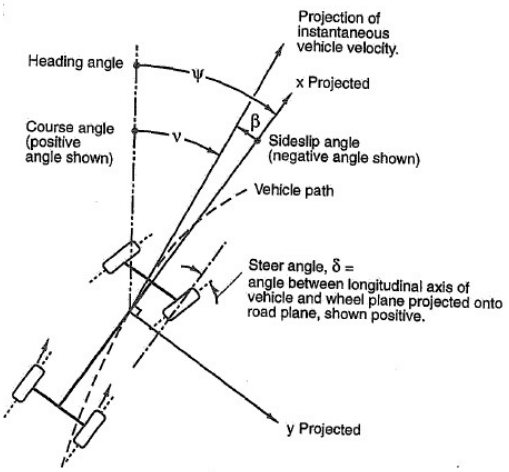

Figure 11: Sideslip angle β of a vehicle [3]

Side-slip angle is another important parameter, as it is yaw rate, to evaluate the stability of a vehicle when performing a curve. Its rate of change, known as sideslip angle rate ($\dot{\beta}$), is normally measured in rad/s or deg/s.

For stability reason is preferred a low value of side slip angle, as near to zero as possible, in order to have a neutral handling when performing a curve.

2.2 Tire Dynamics

The dynamic behaviour of tires is fundamental to properly understand the vehicle comportment. To study it, it is generally considered also a cartesian reference frame for the tires; each tire (generally they are 4) has its own cartesian reference frame. This frame is represented in figure 12.

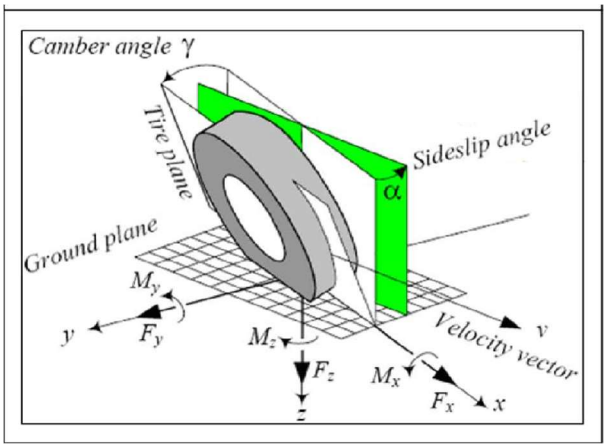

Figure 12: Tire reference frame [5]

The main angles of a tire are:

- α: slip angle (rotation about z-axis)
- γ: camber angle (rotation about x-axis)
- θ: caster angle (rotation about y-axis)

Tire dynamics is the study about the dynamic behaviour of tires; studying the dynamic of tires is fundamental for the complete dynamic study of the vehicle since between tire and ground are exchanged the forces that allows the vehicle to accelerate, brake and turn.

The main parameters of the tires are:

- Slip angle
- Slip ratio
- Cornering stiffness

These parameters are explained in the following paragraphs.

2.2.1 Slip angle

In a tire, the slip angle (known as α) is the angle in between the longitudinal axis of the wheel and the direction in which the wheel is proceeding. The figure 13 represents the slip angle of a general wheel.

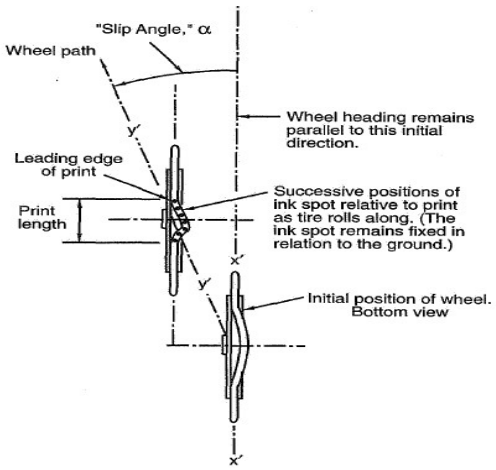

Figure 13: Tire slip angle [3]

The slip angle is normally defined in deg or rad and it's defined as:

$$\alpha = \text{atan}\left(\frac{v_{wheel_y}}{v_{wheel_x}}\right) \tag{13}$$

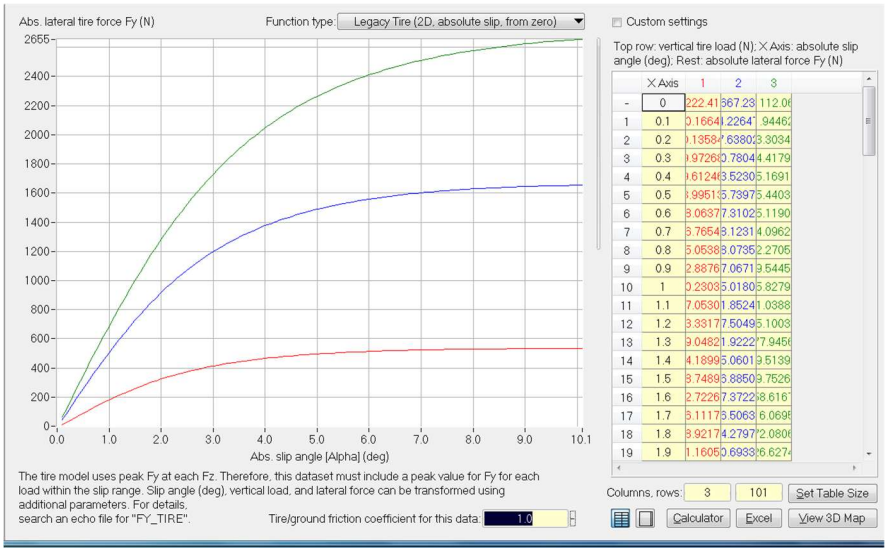

Figure 14: Tire cornering force vs tire slip angle for the Formula SAE vehicle chosen

When the tyre slip angle is different from zero, due to the deformation of the contact zone between tire and ground, a cornering force is exchanged (F_y).

In figure 14, it's presented the lateral force (cornering force) with the variation of the tire slip angle for the chosen vehicle UPM 03E.

The cornering force lies in the contact plane between tire and ground and points perpendicular to the longitudinal axis of the tire. This force increases linearly for low values of slip angles (up to approximately 2 deg, depending on the vertical force applied to the tire) and in the linear region it is proportional to the cornering stiffness of the wheel (measured in N/rad), then it increases non-linearly till a maximum and then decreases after reaching the maximum value.

A value of slip angle different from zero is due to the deformation of the tyre. By analysing the figure 14 it's possible to calculate the rear and front cornering stiffness of tires for the given vehicle. Cornering stiffness states the amount of cornering F_y given by the tires with the variation of tire slip angle α, this is valid only in the linear region of the tire behaviour

The values of the two parameters are computed and listed below:

$$\widetilde{C_{\alpha r}} = 35\,000\ \frac{N}{rad} \tag{14}$$

$$\widetilde{C_{\alpha f}} = 33\,000\ \frac{N}{rad} \tag{15}$$

The value of the cornering stiffness of rear tires is higher because the vertical load on them is higher (as stated in the equations (7) and (8)), so the chart for rear wheels has a higher starting slope.

2.2.1.1 Linear model of tires

As it possible to see in the figure 14 for low values of tire slip angle (α) the curve can be linearly approximated; the starting slope of the curves are equal to the cornering stiffness of the tires $\widetilde{C_{\alpha r}}$ and $\widetilde{C_{\alpha f}}$.

For low values of slip angles (normally lower than 2-3 deg) the curve can be perfectly approximated by this linear model.

In the linear tire model, the cornering force can be thus calculated as:

$$F_{yr} = \widetilde{C_{\alpha r}} * \alpha_r \quad (16)$$

$$F_{yf} = \widetilde{C_{\alpha f}} * \alpha_f \quad (17)$$

Respectively for rear and front tires. In these formulas the value of slip angle must be in rad and the cornering stiffness in N/rad as stated in the equations (14) and (15).

2.2.2 Longitudinal slip ratio

Longitudinal slip ratio is a parameter used to describe the amount of longitudinal slip of the wheels of a vehicle. It's one of the most important parameters in tire dynamics because it permits to comprehend the relationship between the longitudinal deformation of the contact zone of the tyre and the longitudinal forces exerted by the wheels; these forces command acceleration and braking of a vehicle.

Slip occurs when accelerating or braking because of the deformation of the tyre and the spin rates of the wheels is not equal to the one expected considering pure rolling motion; the difference between the theoretical speed of the vehicle and the actual one is considered when computing the slip ratio.

Slip ratio is defined in two different ways depending if the vehicle is accelerating or decelerating. When a vehicle is accelerating, the velocity of the wheel is equal or higher than the one of the vehicle and the slip ratio is defined as:

$$\kappa_{acc} = \frac{\Omega_{\text{wheel}}}{\Omega_{ideal}} - 1 \quad (18)$$

Where:

- Ω_{wheel}: spin rate of the wheel
- Ω_{ideal}: spin rate of the wheel in pure rolling conditions defined starting from the longitudinal speed of the vehicle

When a vehicle is braking, the velocity of the wheel is equal or lower than the one of the vehicle and the slip ratio is defined as:

$$\kappa_{dec} = 1 - \frac{\Omega_{\text{wheel}}}{\Omega_{ideal}} \tag{19}$$

The wheel slip ratio, as defined in the equations (18) and (19), assumes values in between 0 and 1.

The slip ratio is the parameter used to define the longitudinal force exerted by the wheels as it possible to see in the following chart (figure 15). The maximum value of longitudinal force is normally exerted for slip value in between 0,1 and 0,2 depending on the vertical force in the contact path and road characteristics.

In figure 15 it is represented the variation of the longitudinal force exchanged in the contact with the variation of the slip ratio for the given formula SAE vehicle.

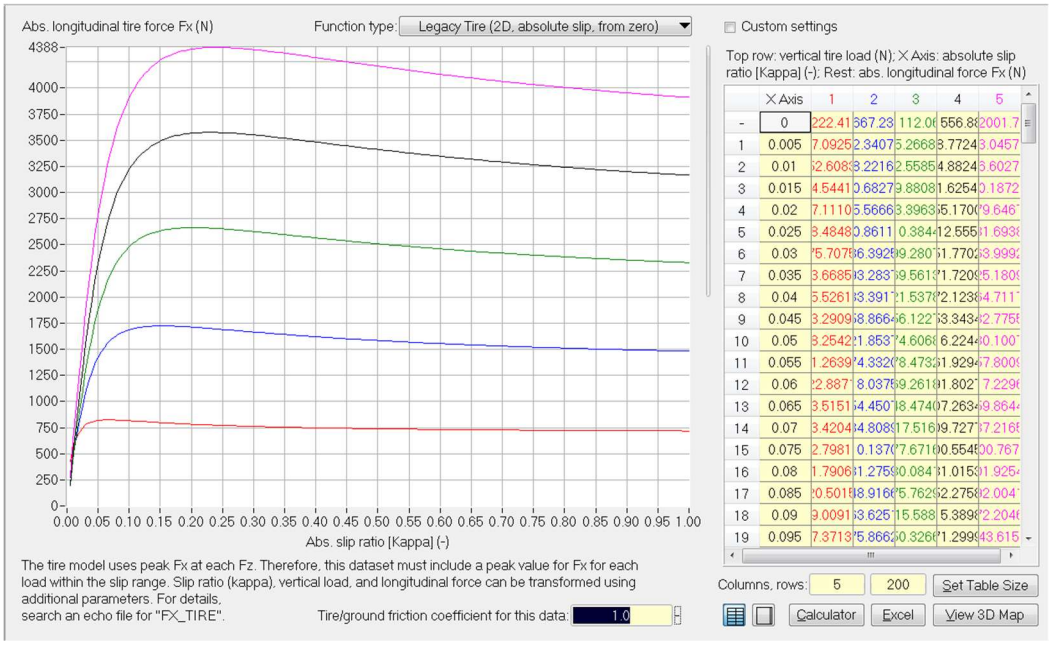

Figure 15: Longitudinal force vs tire slip ratio for the chosen Formula SAE vehicle

Considering a vehicle in constant motion (no acceleration), and taking into account the vertical load distribution between rear and front tires with the equations (7) and (8), it's possible to approximate the slip ratio value for which there's a maximum of longitudinal force exerted. This value is set equal to:

$$\kappa_{\text{lim}} = 0{,}1 \tag{20}$$

When slip ratio exceeds this value the zone is defined instable and slip ratio goes fast to the value 1 guaranteeing only a minimum value of longitudinal force possible

to be exerted. The zone with slip ratio lower than $i_{\lim}$ is considered stable, so it's suggested to work in this zone and limit the slip ratio values that should always be in between 0 and $\kappa_{\lim}$.

2.3 Electric motors

The vehicle is equipped with 4 in-wheel electric motors; these servomotors are supplied by AMK company. In figure 3 it's reported the principal mechanical characteristics of the electric servomotors; in figure 16 it's represented the characteristic curve of the motor.

In nominal operations the servomotor can perform a maximum amount of torque equal to:

$$T_0 = 13{,}8\ N * m \tag{21}$$

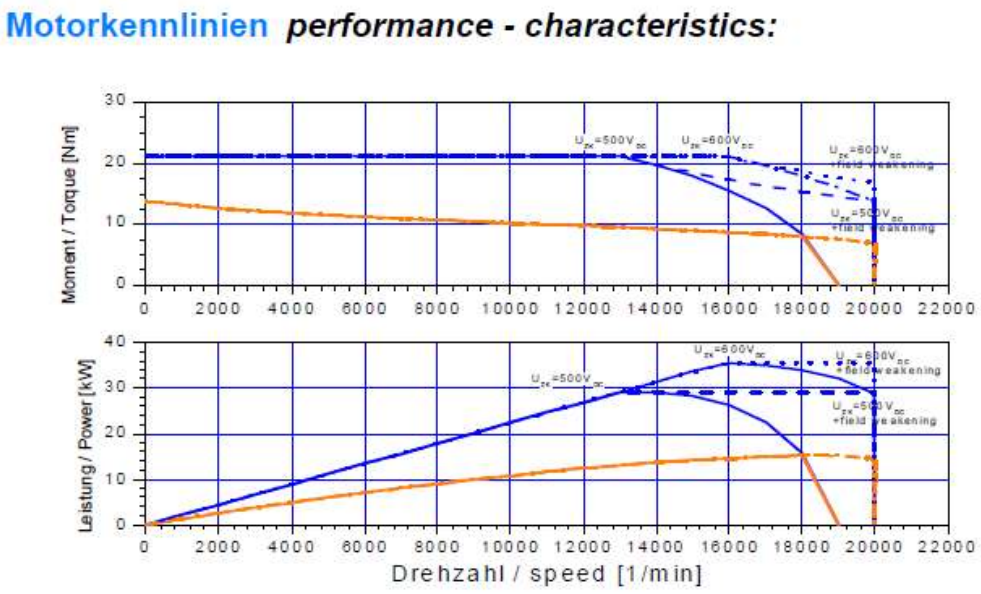

Figure 16: Motor characteristic curves [1]

Knowing the torque curve of the motor with the variation of the spin rates, and roughly approximating it to a linear curve, the curve of the motor can be thus approximated as:

$$T_{wheel} = 13{,}8 - 0{,}00035 * \omega_{motor} \quad (22)$$

The torque is measured in N*m where the ω_{motor} is given in rpm. The motor spin rate can be calculated thanks to the velocity encoder positioned on each motor.

In between each motor and wheel there's a mechanical planetary gear with fixed gear ratio equal to:

$$G_r = 13{,}176 \quad (23)$$

The wheel spin rate can be thus calculated by knowing the motor spin rate in the following way:

$$\omega_{wheel} = \omega_{motor} * G_r \quad (24)$$

The planetary gear is a reducer for spin rate but a multiplier for torque. In fact, the maximum stall torque that can be given to the wheels is equal to:

$$T_{wheelMAX} = T_0 * G_r = 181{,}2\ N * m \quad (25)$$

In the following figure it is represented the constructive features of the motor.

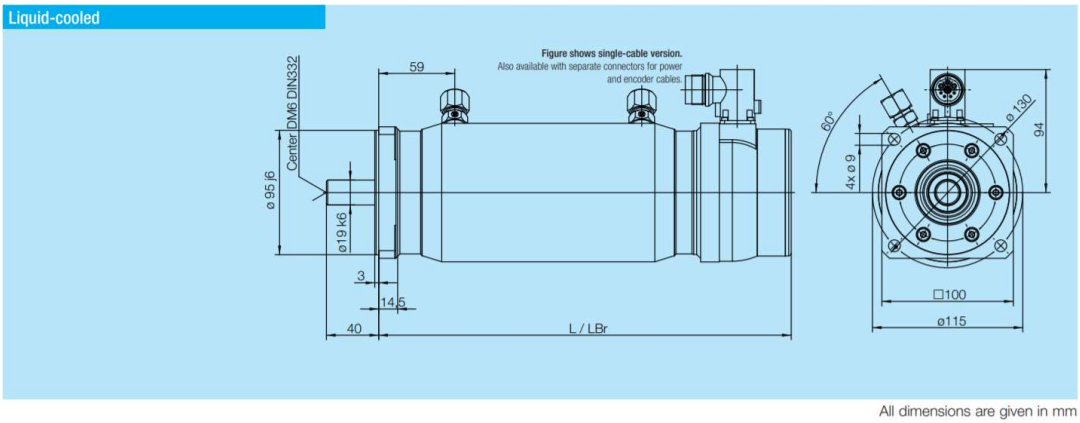

Figure 17: Constructive scheme of the motor [1]

Mechanische Daten *mechanical data:*

Gesamtmasse/motor mass "m":	3,55	kg
Motorträgheitsmoment/inertia "J":	2,74	kgcm²
Mech. zul. Drehzahl/mech. speed limit "Nmax":	20000	rpm
Rundlauf/run out (DIN 42955):	N	
Wuchtgüte/balancing quality:	G2,5	
Schwingstärke/vibration level (DIN ISO 2373):	N	
Passfeder/shaft key:	-	

Figure 18: Mechanical data of the motor [1]

The solution of using this kind of electric servomotors guarantees advantages as high acceleration, efficiency and life.

Due to these features the choice of electric servomotors has been considered the most suitable in the case of in-wheel motor vehicles.

Chapter 3: Torque Vectoring Controller

3.1 TV, state of art

The use of electronic system inside vehicles to guarantee safer conduction has increased its importance during years due also to law requirements in terms of active and passive safety of vehicles and passengers.

The two physical quantities that most affect the stability of a vehicle are the side-slip angle (β) and the yaw rate ($\dot{\psi}$). These two quantities must be properly controlled to ensure the stability of the vehicle, too high values of these two variables make the vehicle unsafe.

The system that is going to be presented in this thesis is based on a yaw rate reference tracking.

Torque vectoring is one of the most important vehicle stability control systems in development nowadays. The use of this system allows to improve and increase the performance of a vehicle in cornering and lateral dynamics without negatively affecting the longitudinal dynamic performance.

The main aim of this thesis is to design a control system to guarantee a better performance of the vehicle when perfoming a turn.

The use of a torque vectoring system allows to properly allocate the torque transmitted to the different wheels of the vehicle conceding a better control of the vehicle in cornering; the correct allocation of torque among the wheels guarantee a vehicle with a faster response to a given value of steer input.

In all-wheel drive vehicles, such as the one that is currently considered, it is possible to distribute instant by instant a different value of torque to each wheel depending on the driving conditions of the vehicle to ensure better control, speed and tracking of the trajectory of the vehicle.

At the end, TV guarantees a vehicle with improved cornering performances. To achieve this objective, it is therefore necessary to develop a control unit (ECU) that, considering the data extracted from the sensors positioned in different part of the vehicle, allows to calculate the exact distribution of torque in wheels.

In the following paragraph it's explained how the TV control structure has been designed with the use of the software Simulink.

3.2 TV Control structure

The control structure has been developed in Simulink; this is a software used for modelling dynamic systems and it's integrated in MATLAB (developed by MathWorks company).

In the figure 19 it's represented the TV control structure designed in MATLAB Simulink.

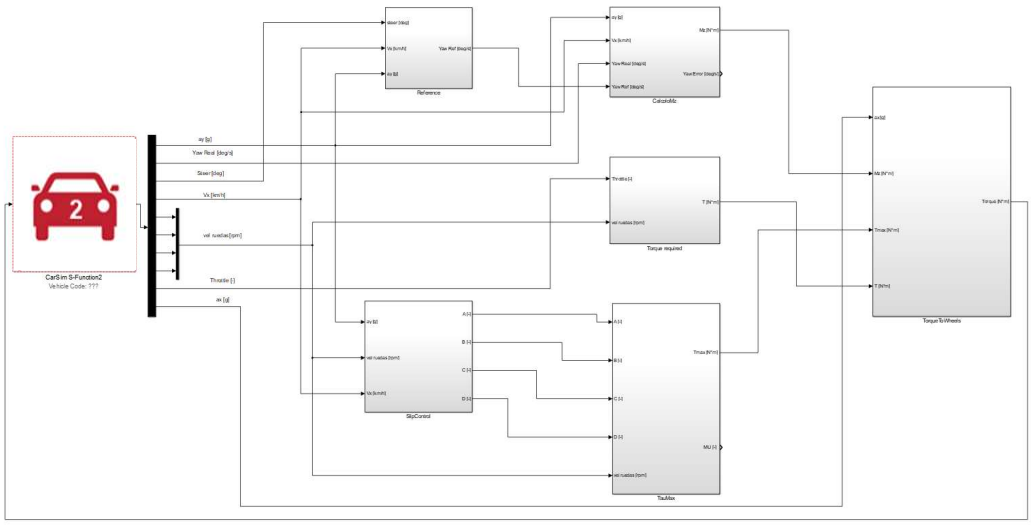

Figure 19: Scheme of the TV control structure in MATLAB Simulink

The control structure is made up of different blocks and then linked to an external simulation software called CarSim (software used to simulate the performance of vehicles) represented in figure 19 with the red car.

The TV control structure represented in figure 19 consists of the following main blocks:

- Yaw Rate Reference
- Yaw Moment Required
- Total Torque Required
- Slip Control
- Maximum Torque Allowed
- Wheel Torque Allocation

3.2.1 Sensors

The control structure, to work, needs information about the vehicle in real time; these data are provided by using different sensors placed inside the vehicle.

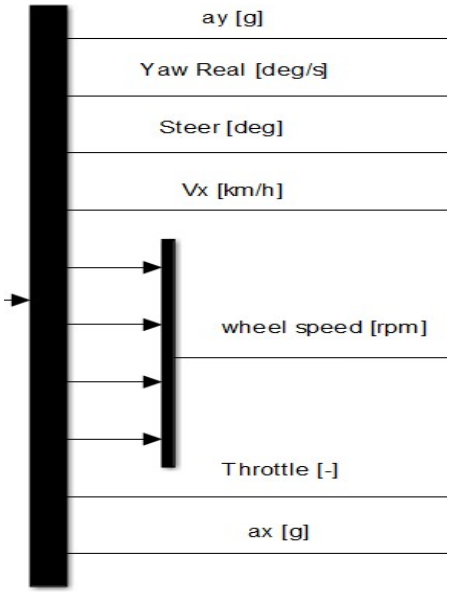

Figure 20: Input state variable for the control system

Sensors are needed to measure the following physical quantities:

- Yaw rate $\dot{\psi}$
- Lateral acceleration a_y
- Longitudinal acceleration a_x
- Steering angle δ
- Wheels speeds ω_{whe}
- Throttle position Tr
- Longitudinal vehicle speed V_x

As it is represented in figure 20.

These parameters can be evaluated by using proper sensors. The sensors used to measure the value of these state variables are the following:

- Accelerometer to evaluate yaw rate and lateral and longitudinal acceleration of CG
- Steering encoder
- Wheel speed encoder (this sensor is present directly inside the motor and the wheel speed can be calculated by knowing the fixed planetary gear ratio G_r in between motor and wheel)
- Throttle position sensor
- GPS to compute the speed of the vehicle

3.2.2 Yaw Rate Reference

Input of the block:

- Steer angle δ [deg]
- Lateral acceleration a_y [g]
- Longitudinal speed V_x [km/h]

Output of the block:

- Yaw rate reference $\dot{\psi}_{ref}$ [deg/s]

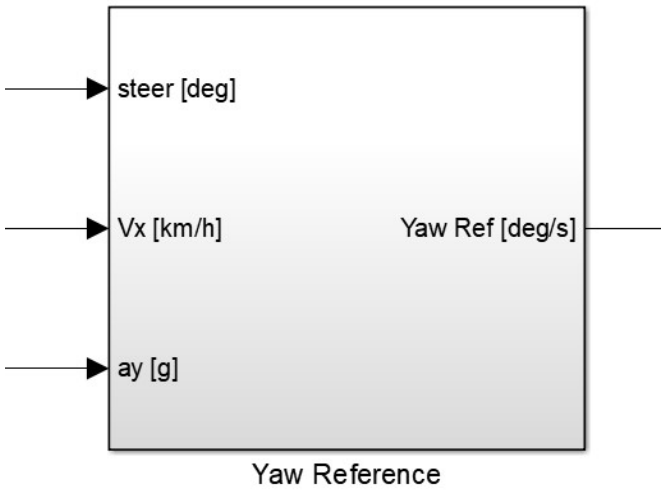

Figure 21: Yaw Reference block inputs and outputs

The aim of this block is computing the value of the yaw rate reference to be ideally followed by knowing the driving condition of the vehicle: steer, speed and lateral acceleration. To be able to calculate this reference value it's needed first to define the vehicle model used and then deriving the final explicit formula.

3.2.2.1 2 DOF Vehicle Model

To completely define the dynamics behaviour of a car a high number of degrees of freedom (DOF) is usually needed. In figure 22 it's represented the complete vehicle model with 14 DOF. Some assumptions can be made to simplify the model and obtain a 2 DOF model of the vehicle. The hypothesis considered are the following:

- Flat road that can be considered a geometrical plane
- Avoid rapid accelerations and braking conditions so to neglect the pitch movement of the vehicle
- Rigid body structure of the vehicle
- Rigid suspensions
- Neglect inertial effects due to roll motion. Racing cars have normally high values of suspension stiffness so that the roll motion can be neglected

- Flat motion of the vehicle
- Rigid steering system
- Small angles of the steering wheels

The total effect of these assumptions is a model with 2 DOF (represented in figure 23), in which the vehicle is represented as rigid body moving in a flat plane.

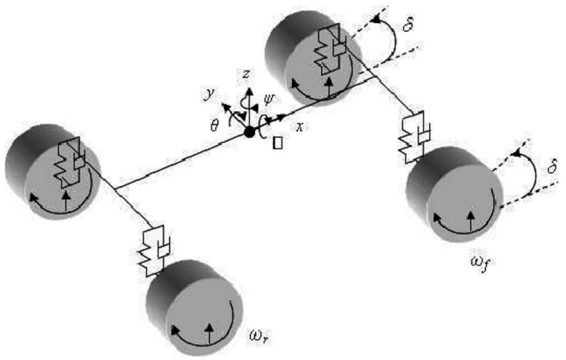

Figure 22: 14 DOF car Model [3]

This 2 DOF model merges the wheels of a common axle in one wheel.

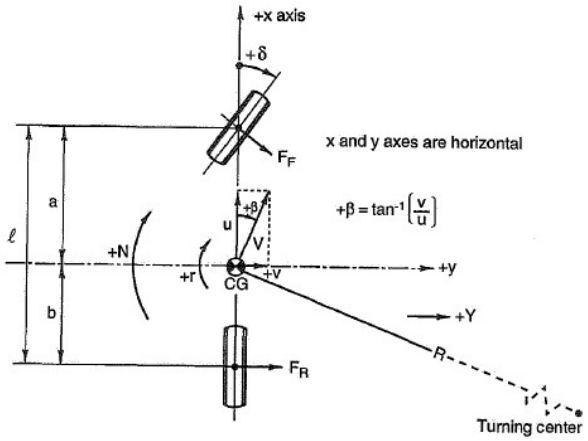

Figure 23: 2 DOF Bicycle Model [3]

It's important to notice that two other important assumptions must be made to properly use this model:

- Equal steering angles of the two front wheels: $\delta = \delta_{fL} \approx \delta_{fR}$

- Small tire slip angles to be able to consider the linear tire model of tires

Fundamental are the passages that merge the characteristics of the two wheels of the same axle. $C_{\alpha r}$ and $C_{\alpha f}$ are the rear and front cornering stiffness of the corresponding tires indicated by the equations (14) and (15). By using the 2 DOF model the characteristics of tires of the same axle must be merged and then the corresponding cornering stiffness of the front and rear axles are defined:

$$C_{\alpha f} = 2 * \widetilde{C_{af}} = 66\,000\ N/rad \tag{26}$$

$$C_{\alpha r} = 2 * \widetilde{C_{ar}} = 70\,000\ N/rad \tag{27}$$

This 2 DOF vehicle model, represented in figure 23, is normally the most used model in literature when the main aim is to study the lateral dynamic of car; this model guarantees a good approximation of the lateral dynamic even if some main dynamic effects of the vehicle are neglected.

The yaw rotation indicated in figure 23 with r will be denoted with $\dot{\psi}$.

Applying the second dynamic law ($\Sigma F = m * a$) to the Y-axis of the vehicle, it's found the following relation:

$$m_{CG} * a_y = F_{yr} + F_{yf} * \cos(\delta_f) \tag{28}$$

With $\delta_f = \delta$, that is the steering angle of the front wheels, being the vehicle a front steering type, and it is supposed equal for the two front tires (which are now merged in only one tire).

F_{yr} and F_{yf} are the cornering lateral forces exerted by the tires. a_y is the lateral acceleration of the vehicle and it can be described as the sum of the variation of the lateral velocity and a term due to the influence of yaw rate and longitudinal velocity:

$$a_y = \dot{v} + \dot{\psi} * u \tag{29}$$

By substituting the equation (29) in the (28), it is obtained:

$$m_{CG} * \left(\dot{v} + \dot{\psi} * u\right) = F_{yr} + F_{yf} * \cos(\delta) \tag{30}$$

To study the lateral dynamics of the car with the 2 DOF model proposed, 2 dynamic equations must be used: the equilibrium of momentum about z-axis (centred on CG) and the equilibrium of lateral forces.

These equations are thus represented in the following system:

$$\begin{cases} m_{CG} * \left(\dot{v} + \dot{\psi} * u\right) = F_{yr} + F_{yf} * \cos(\delta) \\ I_z * \ddot{\psi} = F_{yf} * \cos(\delta) * a - F_{yr} * b \end{cases} \quad (31)$$

By supposing the tire linear model presented in the chapter 2 (valid for low values of tire slip angles), it is possible to state that the lateral force of reaction from the wheels is proportional to the respective slip angle of the wheel (constant cornering stiffness of the wheels).

The slip angles of front and rear tire are:

$$\alpha_f = \delta - \theta_f \quad (32)$$

$$\alpha_r = -\theta_r \quad (33)$$

Thus, the cornering force exerted from the corresponding tire is:

$$F_{yf} = C_{\alpha_f} * \alpha_f = C_{\alpha_f} * (\delta - \theta_f) \quad (34)$$

$$F_{yr} = C_{\alpha_r} * \alpha_r = C_{\alpha_r} * (-\theta_r) \quad (35)$$

From geometrical considerations about the angles:

$$\tan\left(\theta_f\right) = \frac{v + a * \dot{\psi}}{u} \quad (36)$$

$$\tan(\theta_r) = \frac{v - b * \dot{\psi}}{u} \quad (37)$$

The angle of the velocity direction of the wheel with respect with the longitudinal axis of the vehicle is supposed to be small; in this way it's possible to state:

$$\tan(\theta_r) \sim \theta_r \quad (38)$$

$$\tan\left(\theta_f\right) \sim \theta_f \quad (39)$$

And from equations (36) and (37):

$$\theta_f = \frac{v + a * \dot{\psi}}{u} \quad (40)$$

$$\theta_r = \frac{v - b * \dot{\psi}}{u} \quad (41)$$

For the hypothesis made in equations (38) and (39) also the steering angle δ must be small ($\delta = \alpha_f - \theta_f$).

Putting together the equations (34), (35), (40) and (41) it's found the final formula for the cornering force of front and rear axle:

$$F_{yf} = C_{\alpha_f} * (\delta - \frac{v + a * \dot{\psi}}{u}) \quad (42)$$

$$F_{yr} = C_{\alpha_r} * (-\frac{v - b * \dot{\psi}}{u}) \tag{43}$$

By substituting equations (42) and (43) in (31), it's obtained:

$$\begin{cases} m_{CG} * (\dot{v} + \dot{\psi} * u) = -C_{\alpha_r} * (\frac{v - b * \dot{\psi}}{u}) + C_{\alpha_f} * (\delta - \frac{v + a * \dot{\psi}}{u}) * \cos(\delta) \\ I_z * \ddot{\psi} = C_{\alpha_f} * \left(\delta - \frac{v + a * \dot{\psi}}{u}\right) * \cos(\delta) * a + C_{\alpha_r} * (\frac{v - b * \dot{\psi}}{u}) * b \end{cases} \tag{44}$$

Side-slip angle of the vehicle (β) is supposed to be small, so:

$$v = u * \tan(\beta) \Rightarrow \text{small } \beta \Rightarrow v = u * \beta \tag{45}$$

$$\dot{v} = u * \dot{\beta} \tag{46}$$

So, substituting inside the system of equations (44), it is obtained:

$$\begin{cases} m_{CG} * (u * \dot{\beta} + \dot{\psi} * u) = -C_{\alpha_r} * (\frac{u * \beta - b * \dot{\psi}}{u}) + C_{\alpha_f} * (\delta - \frac{u * \beta + a * \dot{\psi}}{u}) * \cos(\delta) \\ I_z * \ddot{\psi} = C_{\alpha_f} * \left(\delta - \frac{u * \beta + a * \dot{\psi}}{u}\right) * \cos(\delta) * a + C_{\alpha_r} * (\frac{u * \beta - b * \dot{\psi}}{u}) * b \end{cases} \tag{47}$$

It is possible to write the system (47) in the following matrix form:

$$\begin{bmatrix} \dot{\beta} \\ \ddot{\psi} \end{bmatrix} = \begin{bmatrix} -1 + C_{\alpha_r} * \frac{b}{m_{CG} * u^2} - C_{\alpha_f} * \frac{\cos(\delta) * a}{m_{CG} * u^2} & \frac{-C_{\alpha_r}}{m_{CG} * u} - C_{\alpha_f} * \frac{\cos(\delta)}{m_{CG} * u} \\ -\frac{C_{\alpha_f}}{I_z} * \frac{a^2}{u} * \cos(\delta) - \frac{C_{\alpha_r}}{I_z} * \frac{b^2}{u} & b * \frac{C_{\alpha_r}}{I_z} - a * \frac{C_{\alpha_f}}{I_z} * \cos(\delta) \end{bmatrix} * \begin{bmatrix} \beta \\ \dot{\psi} \end{bmatrix} + \begin{bmatrix} C_{\alpha_f} * \delta * \frac{\cos(\delta)}{m_{CG} * u} \\ \frac{C_{\alpha_f}}{I_z} * \delta * \cos(\delta) * a \end{bmatrix} \tag{48}$$

By solving this system of ODE we are able to find the reference yaw rate and sideslip angle values.

Constant values that are known from the characteristics of the vehicle are:

- $C_{\alpha r}, C_{\alpha f}, b, a, m_{CG}, I_z$

The values of the sideslip angle and yaw rate depend on the selection of this variables:

- u, δ

So, the two references values depend only on these two variables: velocity and steer input (which were the presented as the inputs of the block in figure 21).

Given the complexity of solving a system of two differential equations for each step of the simulation, to ensure greater speed of calculation, it was decided to use a further simplification of model to calculate the yaw rate reference.

3.2.2.2 Yaw Rate Reference

This simplification is valid for steady state vehicle in high speed cornering.

Considering the linear tire model, it's possible to consider a simplified yaw rate reference value. Applying Newton's second law in lateral direction and considering a small steer angle ($\cos(\delta) \approx \delta$) it is obtained:

$$F_{yr} + F_{yf} = m_{CG} * a_y = m_{CG} * \frac{V_x^2}{R_{turn}} \tag{49}$$

Where $a_y = \frac{V_x^2}{R_{turn}}$ is the centripetal acceleration defined by equation (1).

Since we're considering steady state behaviour in high speed cornering, the value of variation of yaw rate must be null ($\ddot{\psi} = 0$); in this way, the equilibrium equation about z-axis becomes:

$$F_{yf} * a - F_{yr} * b = 0 \tag{50}$$

This equation can be written in the following way:

$$F_{yf} = F_{yr} * \frac{b}{a} \tag{51}$$

Considering linear tire model (F_y varying linearly with tire slip angle α) and the previous equations, it is possible to define the two tires slip angles α_f and α_r:

$$\alpha_f = m_{CG} * \frac{a}{a+b} * \frac{V_x^2}{R_{turn}} * \frac{1}{C_{\alpha_f}} \tag{52}$$

$$\alpha_r = m_{CG} * \frac{b}{a+b} * \frac{V_x^2}{R_{turn}} * \frac{1}{C_{\alpha_r}} \tag{53}$$

From geometrical considerations of the steering behaviour of the vehicle it is possible to state that:

$$\delta = \frac{a+b}{R_{turn}} + \alpha_f - \alpha_r \tag{54}$$

Putting together equation (52) and (53) in (54) the steer equation becomes:

$$\delta = \frac{a+b}{R_{turn}} + \frac{m_{CG}}{a+b} * \frac{V_x^2}{R_{turn}} * (\frac{b}{C_{\alpha f}} - \frac{a}{C_{\alpha r}}) \tag{55}$$

and being K_u the understeer gradient:

$$K_u = \frac{m_{CG}}{a+b} * (\frac{b}{C_{\alpha f}} - \frac{a}{C_{\alpha r}}) \quad (56)$$

the equation (55) becomes:

$$\delta = \frac{a+b}{R_{turn}} + K_u * \frac{V_x^2}{R_{turn}} \quad (57)$$

This equation shows that the steering angle must change with the longitudinal velocity of the vehicle considering constant turning radius depending on the value assumed by K_u. The parameter K_u can generally assumes negative or positive values influencing the way how the steering angle must answer to variation of lateral centripetal acceleration. In figure 24 it's reported a chart with the influence of the understeer gradient on the steer angle in function of the speed of the vehicle.

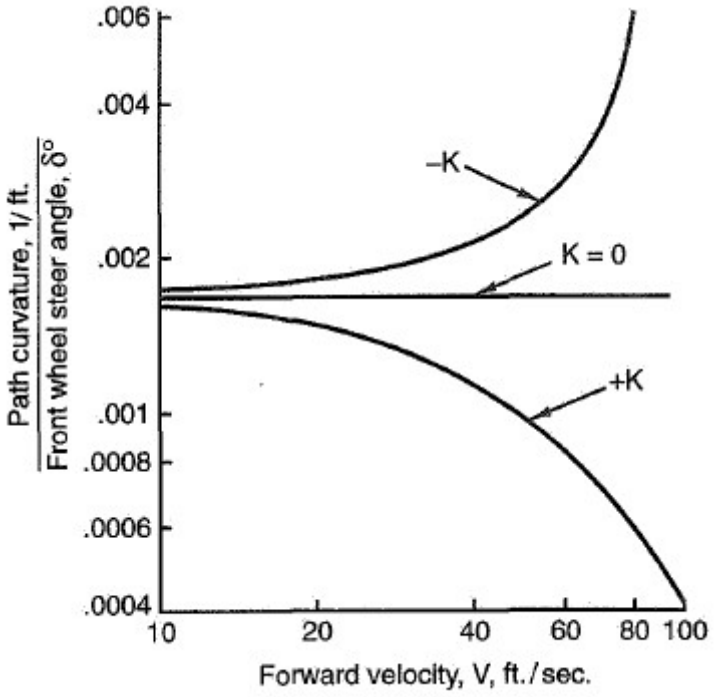

Figure 24: Steer angle in function of speed for different values of understeer gradient [3]

The understeer gradient K_u influences directional behaviour of the vehicle depending on its value; three main cases exist:

- Neutral steer: $K_u = 0$; no change in steer is needed when a_y varies so the steer angle is equal to: $\delta = \frac{a+b}{R_{turn}}$.

- Oversteer: $K_u < 0$; steering angle should decrease with the increase of the longitudinal speed of the vehicle. This behaviour is not stable and for this reason it's not used in normal commercial vehicles.
- Understeer: $K_u > 0$; steering angle should increase while the velocity speed of the vehicle is increasing in constant radius turn. This behaviour is stable and it's the mostly used when designing a commercial vehicle.

The needed characteristics of the vehicle to calculate its understeer gradient are listed below in table 1.

Variable	Value
m_{CG}	219,5 kg
a	0,9 m
b	0,8 m
$C_{\alpha f}$	66 000 N/rad
$C_{\alpha r}$	70 000 N/rad

Table 1: Vehicle parameters to calculate the understeer gradient

It must be added that the cornering stiffness values are considering only the weight force on each wheel without considering any aerodynamic effects that increase the vertical load on the wheels.

$$K_u = -0{,}5 * 10^{-5} \frac{s^2}{m} < 0 \tag{58}$$

This vehicle has so an oversteer behaviour.

It must be added that the presence of the anti-roll bar in the front axle of the vehicle strongly influence the directional behaviour of the car being more understeering; it can therefore be expected that the directional behaviour of the vehicle is at the end understeering.

Let's go back to yaw rate reference calculation. In high speed steady state cornering the yaw rate is defined as:

$$\dot{\psi}_{ref} = \frac{V_x}{R_{turn}} \tag{59}$$

By using the steer angle equation (57) previously defined, it's possible to re-write this equation as a function of the turning radius of the curve:

$$\frac{1}{R_{turn}} = \frac{\delta}{(a+b) + K_u * V_x^2} \tag{60}$$

Substituting it in the equation (59), it's obtained the final yaw rate reference equation that will be used in this TV control system:

$$\dot{\psi}_{des} = \frac{V_x}{L + K_u * V_x^2}\delta \tag{61}$$

For safety reason the value of the reference of yaw rate must be limited to the following value:

$$|\dot{\psi}_{max}| = \left|\frac{a_y}{V_x}\right| \tag{62}$$

So, at the end, the yaw rate reference can be written as:

$$\dot{\psi}_{ref} = \begin{cases} \dot{\psi}_{des} & |\dot{\psi}_{des}| < |\dot{\psi}_{max}| \\ \dot{\psi}_{\max} & otherwise \end{cases} \tag{63}$$

In the figure 25, it's reported the internal structure of this block in Simulink showing how the yaw rate reference value is computed for each step of the simulation

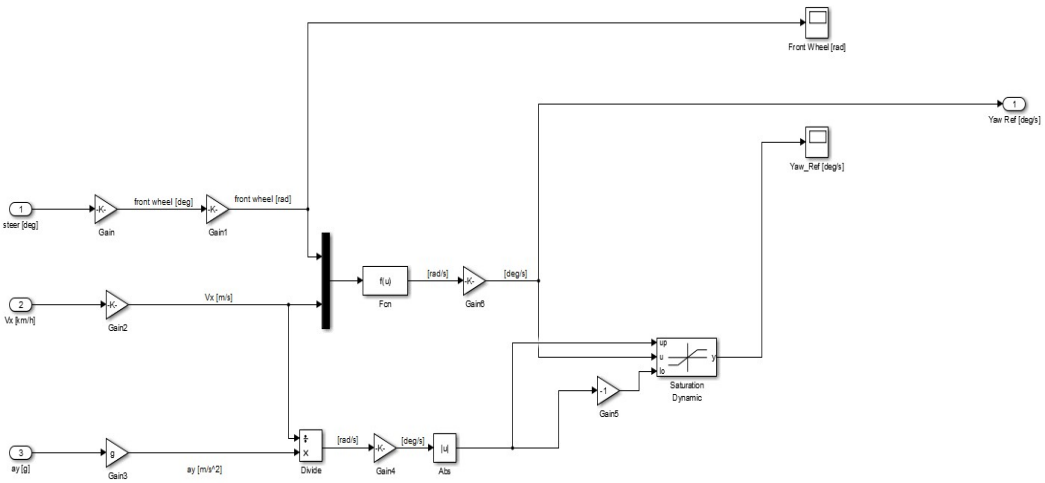

Figure 25: Yaw rate reference control structure

3.2.3 Yaw Moment Required

Input of the block:

- Lateral acceleration a_y
- Longitudinal speed V_x
- Yaw rate real $\dot{\psi}_{real}$
- Yaw rate reference $\dot{\psi}_{ref}$

Output of the block:

- Yaw moment M_z

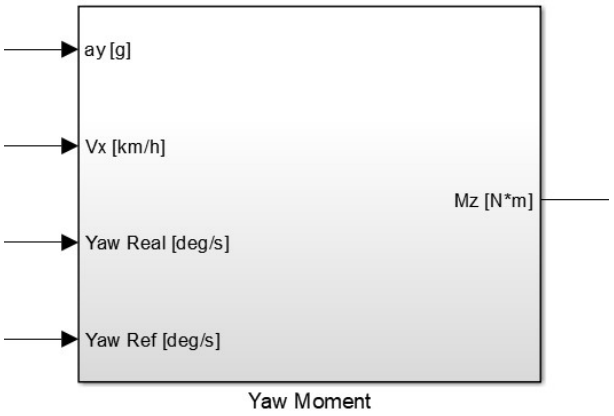

Figure 26: Yaw Moment block inputs and outputs

The aim of this block is to compute the amount of yaw moment needed to balance the difference in yaw rate between the real and the reference value. Every time there's a difference between real and reference yaw rate an amount of yaw moment must be applied to correct this difference; since there's no written relationship between M_z and yaw rate a study with simulations has been carried on.

The yaw moment required can be generated with applying a difference of longitudinal force to the right and left wheels. So, by applying different values of torque to the wheels it's possible to generate a yaw moment in order to guarantee the adjustment needed in the yaw rate.

The equation that links the difference of torque between right and left wheels and the yaw moment so generated is thus presented:

$$M_z = \Delta\tau * \frac{t_f}{2r_{wheel}} \tag{64}$$

By using the simulation software CarSim, with the chosen model of the vehicle, it's applied a difference of torque between left and right wheels in different driving conditions; by varying this amount of $\Delta\tau$ it's possible to compute the variation in value of yaw rate to find a correlation between these two parameters.

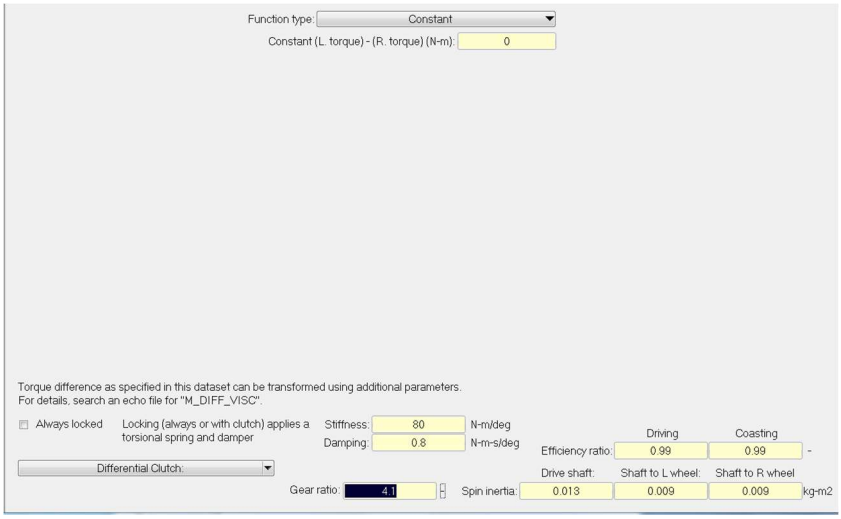

Figure 27: CarSim differential interface

Simulations are carried on with different velocities and different values of steering angle; these are conducted for these values of velocity and steer angle:

- Velocity [km/h]: 20, 30, 40, 50, 60, 70, 90
- Steering angle [deg]: 0, 15, 25, 45, 75, 90, 105, 135, 165, 180

For each different simulation, it's calculated the amount of yaw rate without applying any difference of torque between left and right wheels and then applying this difference equal to 100 N*m. It's thus calculated the slope of the curve of $\Delta\tau$ vs $\Delta\dot{\psi}$ and it's called S; this slope is important to find a correlation between the yaw moment M_z and the error $\Delta\dot{\psi} = \dot{\psi}_{ref} - \dot{\psi}_{real}$.

For each condition of driving (different speed and steering angle) it's calculated the amount of lateral acceleration through the post-processing of the software CarSim. It's decided to use a_y as main parameter to describe this behaviour because

it's easier than using two different parameters (velocity and steering angle); in this way, it's calculated the amount of the slope for different value of a_y.

In the table 2 below the results obtained are reported:

$V_x\ [\frac{km}{h}]$	Steering angle $\delta\ [deg]$	$a_y\ [g]$	Slope of the curve $\Delta\tau\ vs\ \Delta\dot{\psi}$: S_{a_y}
20	-165	-1.18	-25.0
20	-105	-0.72	-61.7
20	-15	-0.125	-88.5
20	15	0.125	-88.5
20	45	0.28	-85.5
20	75	0.5	-80.3
20	90	0.605	-74.3
20	105	0.72	-61.7
20	135	0.95	-43.8
20	165	1.18	-25.0
20	180	1.28	-23.1
30	40	0.58	-49.4
30	45	0.77	-46.2
40	25	0.635	-43.8
70	15	1.06	-33.5

Table 2: Slope of the curve $\Delta\tau$ vs $\Delta\dot{\psi}$ for lateral acceleration different from zero

For same speed of the vehicle and opposite value of steering angle the value of the slope S_{a_y} is the same; in the chart below (figure 29), it is represented the variation of the slope S_{a_y} with the amount of lateral acceleration a_y.

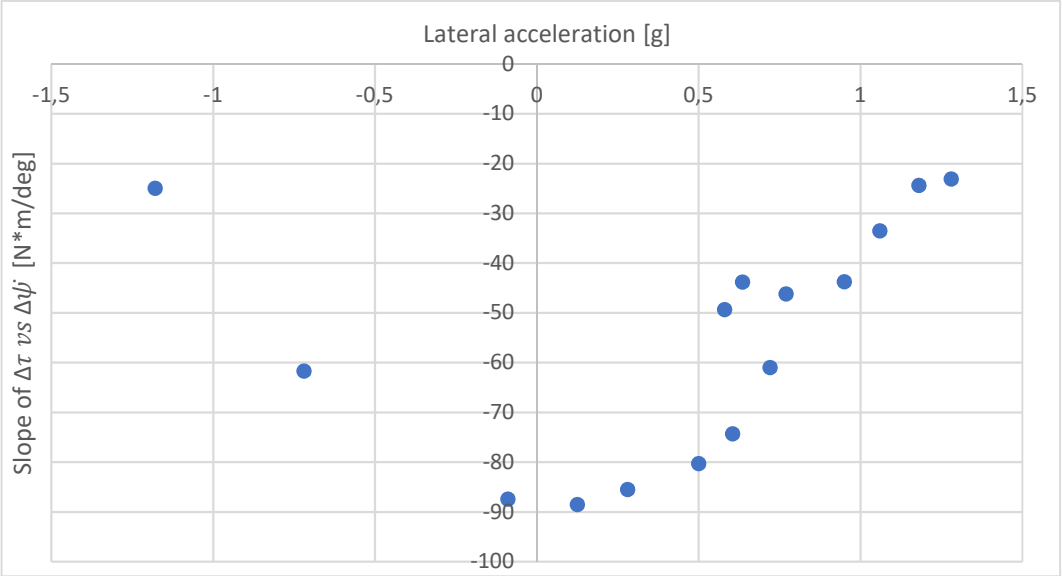

Figure 29: Slope of the curve $\Delta\tau \; vs \; \Delta\dot{\psi}$ for lateral acceleration different from zero vs longitudinal speed of the vehicle

In this way, a relationship between the slope S_{a_y} and the lateral acceleration it's so found approximating it with a linear curve.

$$\text{For } a_y > 0: \qquad S_{a_y>0} = 56{,}6 * a_y - 95{,}6 \tag{65}$$

$$\text{For } a_y < 0: \qquad S_{a_y<0} = -56{,}6 * a_y - 95{,}6 \tag{66}$$

$a_y \; in \; [g]$.

So, during simulations, to calculate the slope S it's used one of the two formulas defined by the equations (65) or (66) depending on the manoeuvre of the vehicle.

The difference of torque between left and right wheel can be thus calculated:

$$\Delta\tau = S * \Delta\dot{\psi} \tag{67}$$

Where S is equal to $S_{a_y>0}$ or $S_{a_y<0}$.

The output of this block corresponds to the yaw moment M_z that must be guaranteed to control the directional behaviour of the car to allows better cornering performance of the vehicle.

In figure 29 it's represented the structure of the yaw moment block in Simulink.

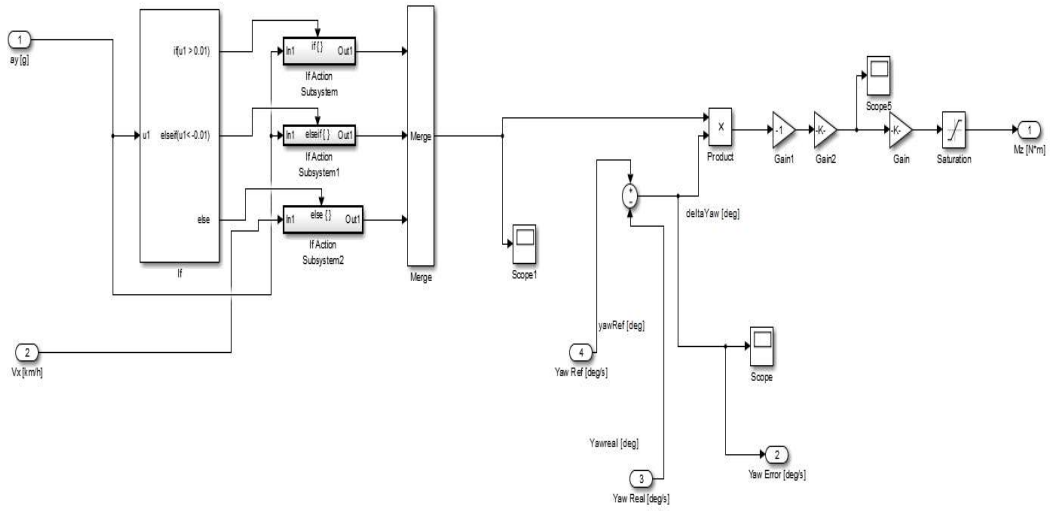

Figure 28: Yaw moment required control structure

3.2.4 Torque required

Input of the block:

- Throttle Tr
- Wheels speeds ω_{wheel}

Output of the block:

- Torque required T_{tot}

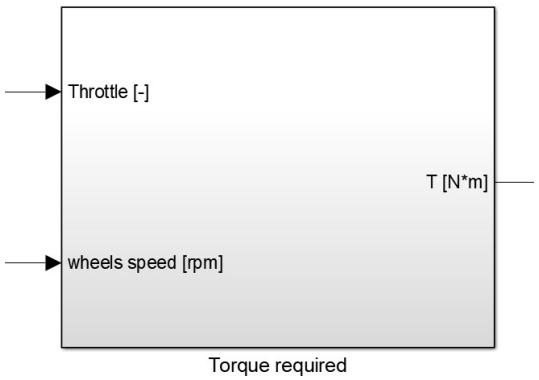

Figure 29: Torque required block inputs and outputs

The torque required by the driver is computed considering the curve of the electric motor.

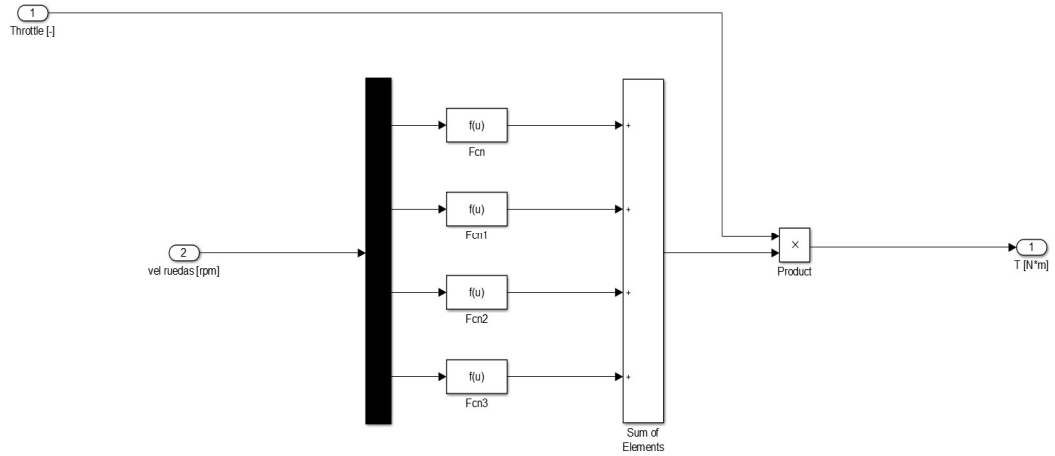

Figure 30: Torque required control structure

Through the electric motor curves, represented in equation (22), the maximum torque available for each wheel is calculated considering its instantaneous spin rate. Then, all the maximum torques for each wheel are summed up and multiplied for the value of throttle derived by the sensor (going from 0 to 1). In this way the amount of total torque required by the driver is computed.

In figure 31 it's represented the structure of this block.

3.2.5 Slip control

Input of the block:

- Longitudinal speed V_x
- Wheels speeds ω_{wheels}

Output of the block:

- Boolean variables: A, B, C, D

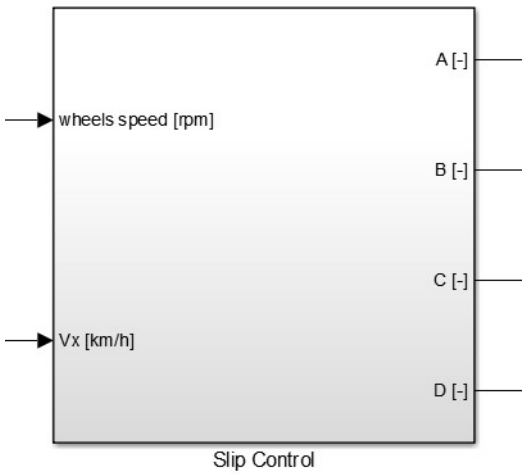

Figure 31: Slip control block inputs and outputs

For each wheel it is calculated the amount of longitudinal slip with the equations (18) or (19) depending if the vehicle is accelerating or braking; the output value for each wheel is then converted in Boolean variable as explained here below.

If the value of longitudinal slip overcomes the value of $\kappa_{\lim} = 0{,}1$ (this value is explained in the paragraph "Slip ratio" in Chapter 2, equation (20)) then the output value is 1; if not, the corresponding output value is 0.

At each wheel is assigned a corresponding letter:

- Front left: A
- Front right: B
- Rear left: C
- Rear right: D

An example is here reported (κ is the longitudinal tire slip):

$$\kappa_{fL} = 0{,}12$$

$$\kappa_{fR} = 0{,}03$$

$$\kappa_{rL} = 0{,}15$$

$$\kappa_{rR} = 0{,}08$$

The corresponding output values for this block would be:

$$A = 1$$

$$B = 0$$

$$C = 0$$

$$D = 1$$

The structure of this block is reported in figure 33.

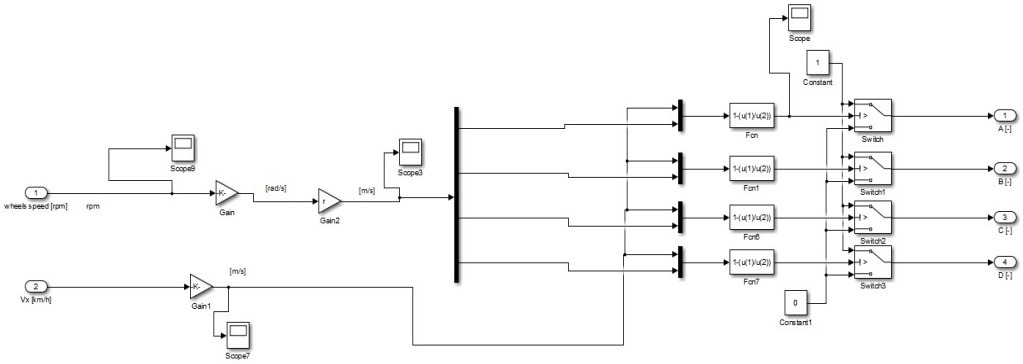

Figure 32: Slip control structure

3.2.6 Maximum Torque Allowed

Input of this block:

- Boolean variables: A, B, C, D
- Wheels speeds ω_{wheels}

Output of this block:

- Maximum wheels torque T_{max}

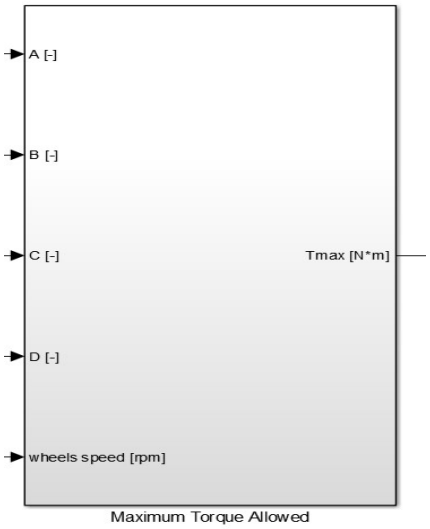

Figure 33: Maximum torque allowed block inputs and outputs

The aim of this block is to calculate the maximum torque allowed in each wheel considering the slipping condition and the maximum torque than can be given by the motor considering its spin rate.

In figure 35 it's reported the internal structure of this block.

At the start of the simulation (time=0) the maximum torque allowed for each wheel is equal to the one due to the motor curve (depending only on the motors spin rate). Then, as input of this block, the 4 Boolean variables are evaluated to ensure that there's or not slip on each single wheel. Slip condition on wheels must be avoided because it causes the tires to work at a low value of adherence coefficient with the ground and causing driving instability and unsafety.

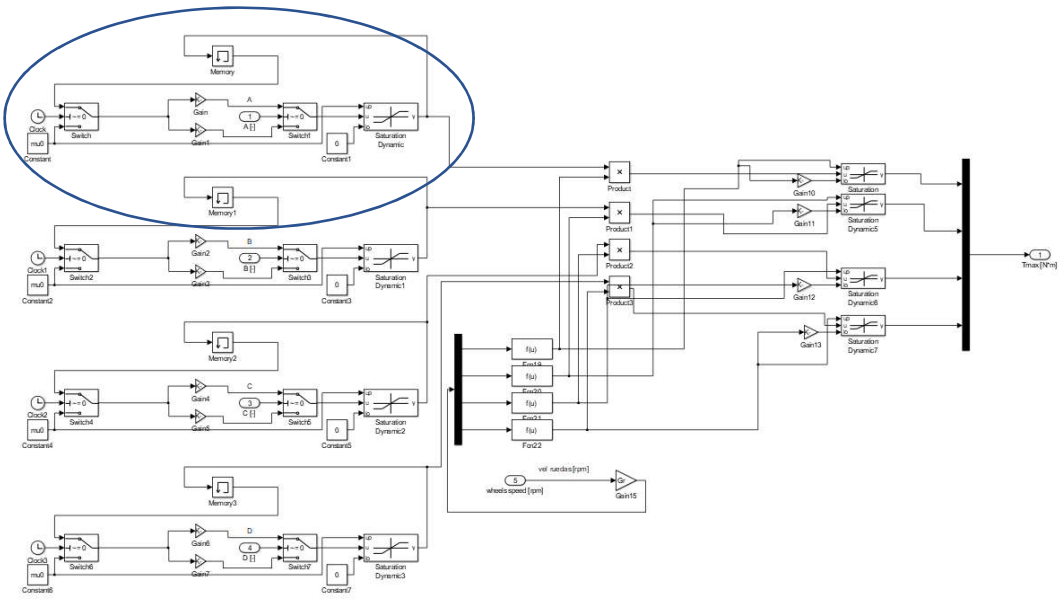

Figure 34: Maximum torque required control structure

A cycle of control is built up (blue circle in figure 25). Let's take for example the front left wheel (its assigned Boolean variable is A) and its zoomed control cycle is reported here below in figure 36.

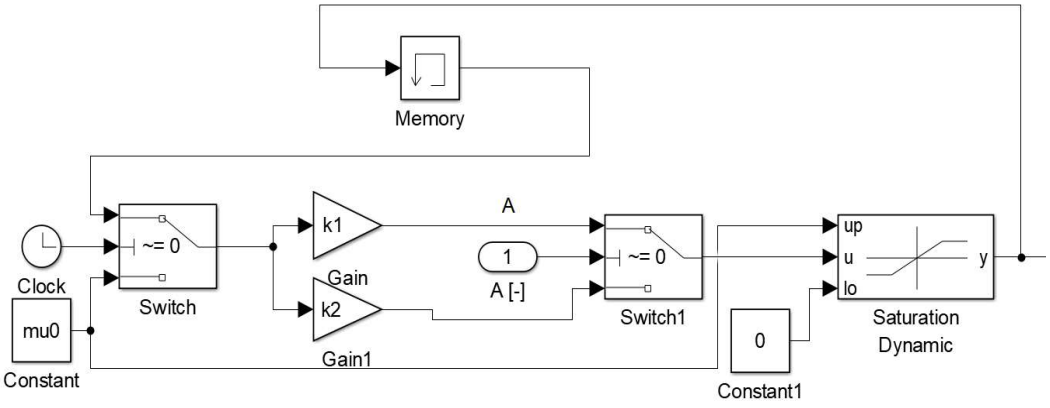

Figure 35: Zoom of a part of the maximum torque required control structure

If the value of the Boolean variable (A in this case) is equal to 1, the idea is to limit the maximum torque possible to this wheel by multiplying it for a factor lower than 1; instead, if the value is 0 (no slip) the maximum torque is multiplied for a factor higher than 1 till it reaches the maximum value possible (that is equal to maximum torque possible given by the motor, depending on its spin rate).

So, if the Boolean variable is equal to 1 the maximum torque is decreased by multiplying it by a factor $k_1 = 0{,}999$.

Instead, if the Boolean variable is equal to 0 the maximum torque is increased by multiplying it by the factor $k_2 = 1{,}001$.

These factors are chosen as close as possible to 1 to guarantee a smooth variation of torque in between two-time steps of the simulation.

Acting in this way it's possible to control independently the level of slip of the four tires allowing the vehicle to be driven safely and faster.

3.2.7 Wheels Torque Allocation

Input of the block:

- Longitudinal acceleration a_x
- Yaw moment M_z

- Maximum wheels torque T_{max}
- Torque required T_{tot}

Output of the block:

- Wheels allocated torque T

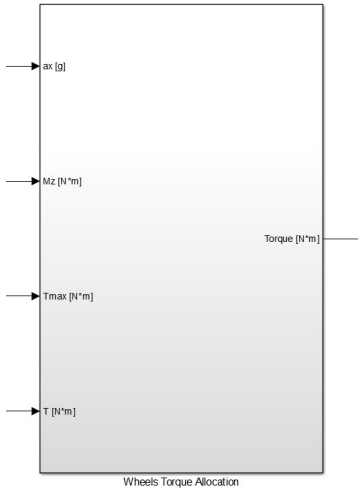

Figure 36: Wheel torque allocation block inputs and outputs

This is the final block where all the information of the other blocks converges to calculate the best possible wheels torque allocation for each step of the simulation carried on.

The longitudinal acceleration is needed to compute the longitudinal load transfer that allows to assign the torque proportionally to the vertical load on the two axles.

The torque is laterally distributed depending on the yaw moment request to be balanced.

The starting equations to compute the torque allocation are the following:

$$\begin{cases} T_{tot} = \tau_{fL} + \tau_{fR} + \tau_{rL} + \tau_{rR} \\ \dfrac{\tau_{fL} + \tau_{fR}}{\tau_{rL} + \tau_{rR}} = \dfrac{m_{CG}g - \dfrac{m_{CG}g}{a+b} * (a + \dfrac{a_x}{g}H)}{\dfrac{m_{CG}g}{a+b} * (a + \dfrac{a_x}{g}H)} \\ \tau_{fR} - \tau_{fL} = \dfrac{M_{zf}}{G_r * t_f} * r_{wheel} \\ \tau_{rR} - \tau_{rL} = \dfrac{M_{zr}}{G_r * t_f} * r_{wheel} \end{cases} \quad (69)$$

By solving this system, it is possible to find a closed form solution that allows to simply evaluate the amount of torque to be distributed to the four wheels.

The first equation states that the sum of all the torques must be equal to the torque required by the driver; the second one affirms that the ratio of the total torque on the front and rear axles must be proportional to the amount vertical load on the respective axle.

Indicating with the constant value K_{Mz} the term $\frac{m_{CG}g-\frac{m_{CG}g}{a+b}*(a+\frac{a_x}{g}H)}{\frac{m_{CG}g}{a+b}*(a+\frac{a_x}{g}H)}$, the second equation of the system (69) becomes:

$$\frac{\tau_{fL}+\tau_{fR}}{\tau_{rL}+\tau_{rR}}=K_{Mz} \tag{70}$$

The third and fourth equation of the system specify that the difference of torque between left and right side must be proportional to the required yaw moment to be exerted.

M_{zr} and M_{zf} are the yaw moment required respectively for the rear and front axles; the values of the parameters M_{zr} and M_{zf} can be calculated by solving the following system of equations:

$$\begin{cases} M_{zr}+M_{zf}=M_z \\ \dfrac{M_{zf}}{M_{zr}}=K_{Mz} \end{cases} \tag{71}$$

In this way the total yaw moment required is divided into the two axles proportionally to the amount of vertical load of each axle.

The described system of equation (69) is formed by four first order linear equations. The unknown parameters to be computed are the four torques values ($\tau_{fL},\ \tau_{fR},\ \tau_{rL},\ \tau_{rR}$); by using simply mathematical tools, it is possible to re-write the four equations making the four torques terms explicit and obtaining the following closed form solution:

$$\tau_{fL}=\frac{K_{Mz}*T}{2*(K_{Mz}+1)}-\frac{M_{zf}}{2F} \tag{72}$$

$$\tau_{fR}=\tau_{fL}+\frac{M_{zf}}{F} \tag{73}$$

$$\tau_{rL}=\frac{T}{2}-\frac{K_{Mz}*T}{2*(K+1)} \tag{74}$$

$$\tau_{rR} = \tau_{rL} + \frac{M_{zr}}{F} \tag{75}$$

Where F is defined as:

$$F = G_r * \frac{t_f}{r_{wheel}} \tag{76}$$

With the four equations ((72), (73), (74) and (75)) presented above it's possible to compute the wheels torque allocation for each step of the simulation.

3.3 Weak points of the presented TV controller

The proposed structure built in Matlab Simulink is based on some assumptions that make the model valid to be used only in particular driving manoeuvres. The assumptions made to design the controller are resumed here below:

- Flat road that can be considered a geometrical plane
- Avoid rapid accelerations and braking conditions so to neglect the pitch movement of the vehicle
- Rigid body structure of the vehicle
- Rigid suspensions
- Neglect inertial effects due to roll motion. Racing cars have normally high values of suspension stiffness so that the roll motion can be neglected
- Flat motion of the vehicle
- Rigid steering system
- Small angles of the steering wheels
- Small tire slip angles
- Sideslip angle of the vehicle (β) is supposed to be small

Due to these assumptions the model designed can be used in manoeuvres that guarantee the following features:

- Small tire slip angles

- Small lateral acceleration

This means that the model can be correctly used to simulate manoeuvres that do not pull the vehicle to its adherence limits and with high ground adherence coefficient.

Chapter 4: Simulation Analysis

To simulate the behaviour of the vehicle the commercial software CarSim has been used in a co-simulated environment with MATLAB Simulink; the purpose of this thesis is to evaluate the advantages carried on by using a TV controller, as the one proposed in chapter 3. The simulations will be carried on in 2 different conditions comparing the results obtained by using the proposed TV controller with the case of the torque equally distributed among the four wheels of the vehicle.

4.1 CarSim

CarSim is a commercial software that can predict the performances of vehicles in response to the commands of the driver (steering, throttle and braking) in a chosen simulated environment (street geometry, conditions and adherence coefficient).

This software is used for research reason in a lot of automotive companies because its mathematical models guarantee to simulate physical tests in a faster way. One of the main advantages is the possibility to simulate the behaviour of a designed vehicle that has not been produced yet.

This software can be properly used to simulate the manoeuvrability, cornering behaviour, braking and acceleration of a vehicle; on the other hand, it does not have components that can consider the fatigue and high-frequency vibration behaviour. This software so can perfectly fit the requests of this thesis work where the main aim is to simulate the lateral and cornering behaviour of the vehicle.

The CarSim model is constructed to be able to work with other softwares (such as Simulink). The vehicle math model in CarSim can control all different features such as: driver control, road geometry and friction, suspensions, steering system, brake system, tire models and powertrain.

CarSim uses ordinary differential equations (ODEs) to simulate the dynamics of the vehicle. The number of differential equations and state variables depend on the model; the basic CarSim model uses 89 ODEs and about 250 state variables.

4.2 Co-simulation

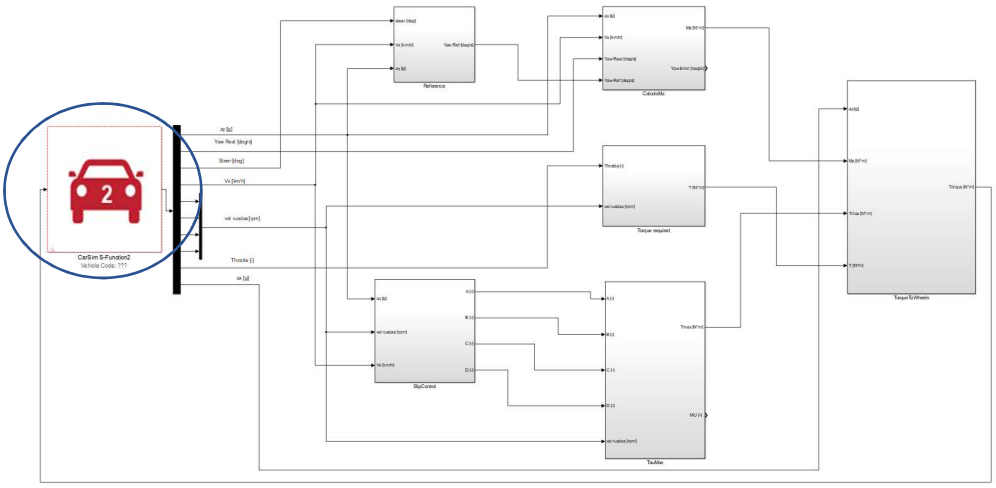

Figure 37: Co-simulation of CarSim inside Simulink

To study the dynamic behaviour of the vehicle a co-simulated environment has been done between the sotwares CarSim and Matlab Simulink. In figure 38 it's represented the co-simulated environment in the Simulink software interface.

In the blue circle it's represented the CarSim block inside the whole Simulink interface built from different blocks explained in the chapter 3.

4.2.1 Cosimulation features

To be able to co-simulate in between the two presented software it's necessary first define the time step of the simulation carried on. In CarSim the time step it's set equal to 0,001 s; as suggested from the manual, the Simulink time step is set equal to a half of the one of CarSim being so equal to 0,0005 s. The integration method chosen for co-simulation uses 2 updates per step. In figure 39 it's represented the time step set.

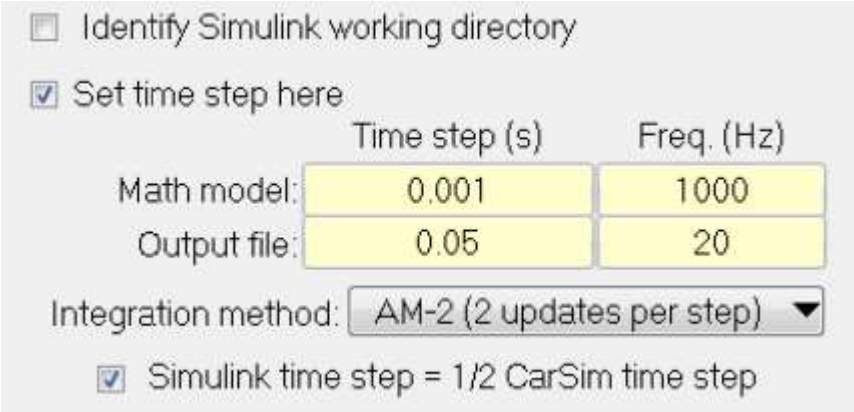

Figure 38: Time step of the simulation

A VS solver runs in Simulink with an S-Function, represented in figure 40, that uses import and export state variables to co-simulate with the model built in MATLAB Simulink.

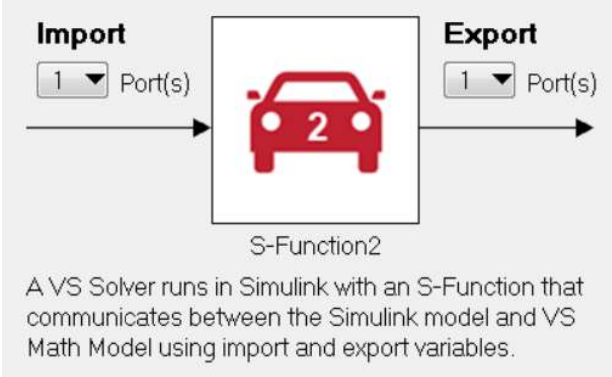

Figure 39: Import and export of CarSim solver

The import and export state variables used to run the simulation are reported in table 3.

	Import	Export
1	Front Left Wheel Torque [N*m]	Lateral Acceleration of CG [g]
2	Front Right Wheel Torque [N*m]	Yaw Rate [deg/s]
3	Rear Left Wheel Torque [N*m]	Steer Angle [deg]
4	Rear Right Wheel Torque [N*m]	Longitudinal speed of CG [km/h]
5	-	Front Left Wheel Spin Rate [rpm]
6	-	Front Right Wheel Spin Rate [rpm]
7	-	Rear Left Wheel Spin Rate [rpm]
8	-	Rear Right Wheel Spin Rate [rpm]
9	-	Throttle [-]
10	-	Longitudinal Acceleration of CG [g]

Table 3: Import and export of CarSim solver

4.3 Vehicle parameters

In this paragraph the main parameters of the vehicle are reported in the following tables. In table 4 and 5 are reported respectively the parameters of the electric motors and of the vehicle.

Parameter	Symbol	Value
Continuous stall torque	T_0	13,8 N*m
Maximum torque	T_{max}	21 N*m
Rated torque	T_n	9,8 N*m
Rated power	P_n	12,3 kW
Rated speed	n_n	12000 rpm
Theoretical no-loaded speed	n_0	18617 rpm

Table 4: Motor parameters

Parameter	Symbol	Value
Sprung mass of the vehicle	m	165 kg
Unsprung mass	m_u	
Length from CG to front axle	a	0.9 m
Length from CG to rear axle	b	0.8 m
Distance between wheels	t_f	1,225 m
Moment of inertia about z-axis	I_z	90 $kg * m^2$
Unloaded tire radius	r_{wheels}	0,265 m
Height of the CG of the vehicle	h_{CG}	0,225 m
Gear wheel ratio	G_r	13,176
Steer ratio	S_r	4,478
Front axle equivalent cornering stiffness	$C_{\alpha f}$	66 000 N/rad
Rear axle equivalent cornering stiffness	$C_{\alpha r}$	70 000 N/rad

Table 5: Vehicle main parameters

The tires used from the Formula SAE vehicle UPM 03E are of the slick type from the company HOOSIER. These tires have a rim diameter equal to 10” (0,254 m) and an example of them is reported in figure 41.

Figure 40: Hoosier Formula SAE slick tire [6]

They are slick racing tires used generally by the major part of the cars participating at the Formula SAE competition. For slick tires used in formula cars the maximum

adherence coefficient can vary in between the range 1,4 and 1,7 depending on many external parameters such as temperature and conditions of the ground.

In the simulations carried on in the following part of the thesis it has been decided to use an adherence coefficient equal to 1 considering dry asphalt not in perfect conditions.

4.4 Simulations

Simulations are carried on in the co-simulated environment between CarSim and MATLAB Simulink in 2 different driving conditions. First two manoeuvres at constant steer are carried on with two different steer input; these simulations are chosen to evaluate the cornering behaviour of the vehicle. Then, a double lane change (DLC) manoeuvre is analysed to evaluate the effectiveness of the controller in such a complex manoeuvre.

The main characteristics of the simulations carried on are reported in table 6.

Simulations	Steering [deg]	Throttle [%]	Initial Velocity [km/h]	Adherence Coefficient [-]
#1 Constant Steer Driving	10	50	0.00	1.00
#2 Constant Steer Driving	20	50	0.00	1.00
#3 DLC	Closed-Loop	100	0.00	1.00

Table 6: Simulations characteristics and input

4.5 Simulation: CONSTANT STEER DRIVING

In this simulation it's used a constant steering wheel input on the vehicle to simulate and evaluate the vehicle cornering behaviour and performance. The simulation is carried on with a beginning initial speed equal to zero that will be increased during the simulation since the throttle pedal is kept constant equal to a 50% of the maximum of the throttle stroke; so, the required power and torque by the driver are half of the full capacity of the vehicle.

This cornering test is performed two times: first with a steer input equal to 10 deg and then with 20 deg. The steer input is kept constant all over the simulation.

4.5.1 #1 Constant Steer Input of 10°

This simulation is performed with a constant steer input equal to 10 deg. The results of the simulations are presented and commented here below. The simulation ends when the vehicle reaches a value of longitudinal speed of 100 km/h.

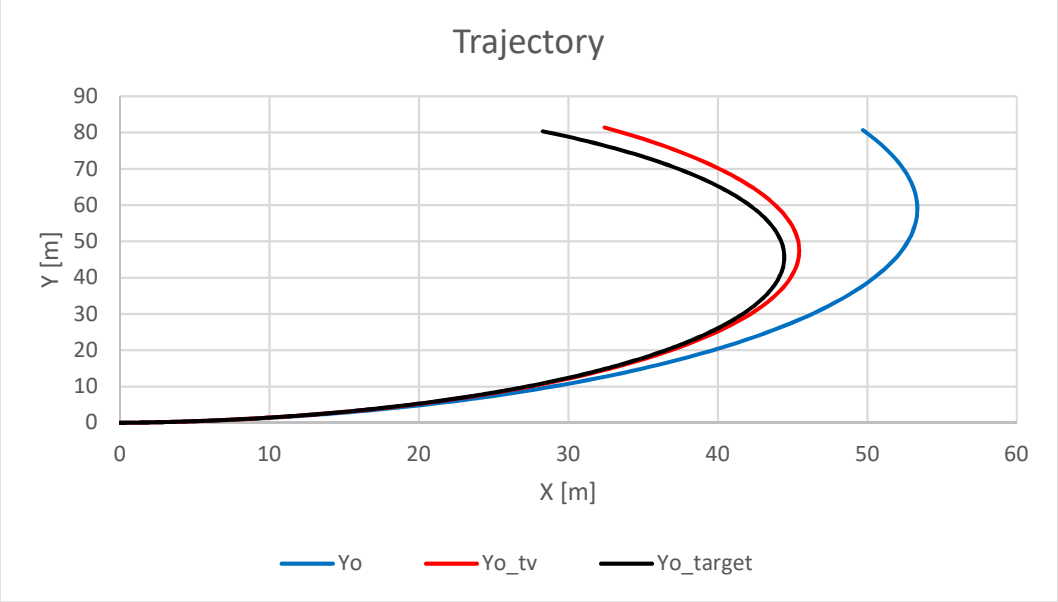

Figure 41: Plot of the vehicle trajectory for a constant steer input of 10°

In figure 42 the trajectory of the vehicle is reported in three different cases. The black curve represents the ideal vehicle path performed at low velocity with the constant steer input of 10°. The other two curves indicate the trajectory when using the TV controller (red curve) and without the designed controller (blue curve). When the vehicle runs without TV the total required torque, calculated by means of the throttle pedal, is equally divided among the four wheels of the vehicle.

As it possible to see the vehicle with TV follows better the ideal target curve. Due to the continuous increase in the longitudinal speed of the vehicle, represented in the figure 43, both the trajectories with and without TV tend to move away from the reference target curve (represented in black in figure 42) but the vehicle with TV has a better response since can allocate more torque to the external wheels guaranteeing a trajectory with a smaller cornering radius.

The longitudinal velocity of the vehicle can be considered equal in both the two cases, as stated in figure 43.

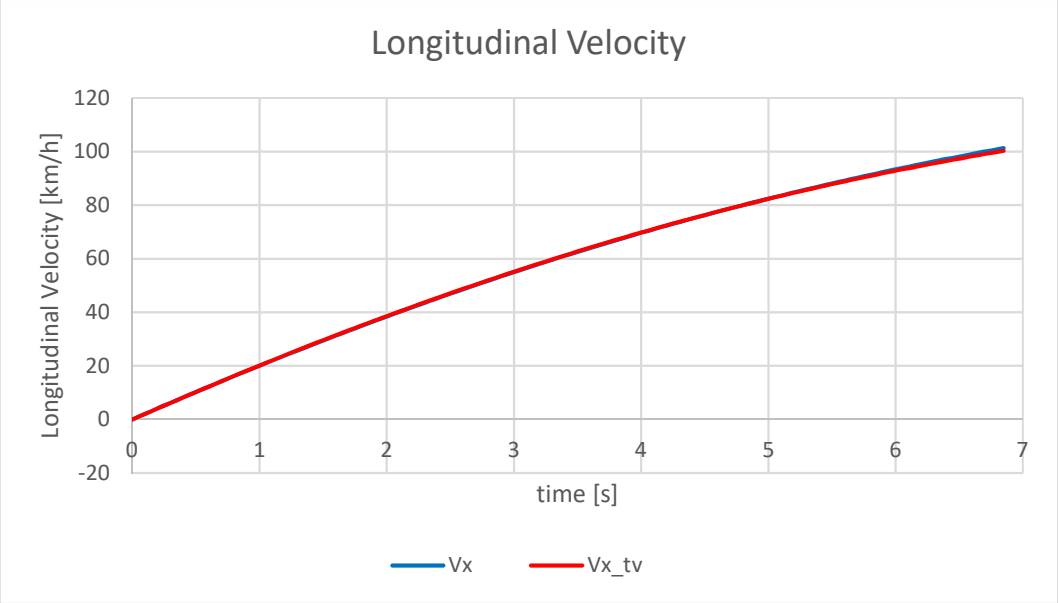

Figure 42: Plot of the vehicle longitudinal speed for a constant steer input of 10°

As it is possible to see in figure 42, the vehicle with and without TV has an understeer behaviour even if the understeer gradient calculated with the equation (56) states that the vehicle has a oversteer directional behaviour. This is due to the presence of the anti-roll bar in the front axle of the vehicle that influences the directional behaviour of the vehicle making it more understeering. Since the value

calculated in equation (58) stated that the vehicle had a slightly ideal oversteering behaviour, considering the presence of the anti-roll bar it can be expected that at the end in real driving condition the vehicle assumes an understeer behaviour. In figure 42 it's possible to see how the vehicle with TV has less understeer behaviour than the case without TV.

In order to evaluate the deviation from the target ideal curve and the effectiveness of the proposed control strategy it's decided to use the parameter NRMSD (Root Mean Square Deviation) to evaluate the deviation of the two trajectories from the ideal one (represented in black in figure 42); this parameter is used to evaluate the deviation of a curve from a target one and it's defined by the following formula:

$$RMSD = \sqrt{\frac{\sum_{i=1}^{n}\left(Y_i - Y_{target_i}\right)^2}{n}} \tag{77}$$

Where n is the number of time step of the simulation. The parameter NRMSD (Normalized RMSD) is defined as:

$$NRMSD = \frac{RMSD}{Y_{max} - Y_{min}} \tag{78}$$

The values of deviation are then calculated and reported in table 7.

DEVIATION TABLE	TV	NO TV
NRMS	**1,99**	**10,22**
NRMSD	**0,025**	**0,128**

Table 7: Normalized root mean square deviation for a constant steer input of 10°

The result of table 7 were intuitable considering figure 42, but it has been preferred giving a numerical value to the deviation of the trajectories. As it's possible to see in table 8 the NRMSD of the vehicle with TV is about 5 times higher than the one with TV.

In figure 44 it's represented how the torque is allocated among the four wheels. It can be seen how the torque is distributed: since the vehicle is longitudinally accelerating, considering the longitudinal transfer load, more torque is applied to the rear wheel with respect to the corresponding front wheel. Since the turn is

performed to the left and the vehicle tends to have an understeer behaviour, moving away from the ideal trajectory, more torque is applied to the right wheels. That's the explanation why the vehicle with TV has a less understeer behaviour with respect to the vehicle without TV.

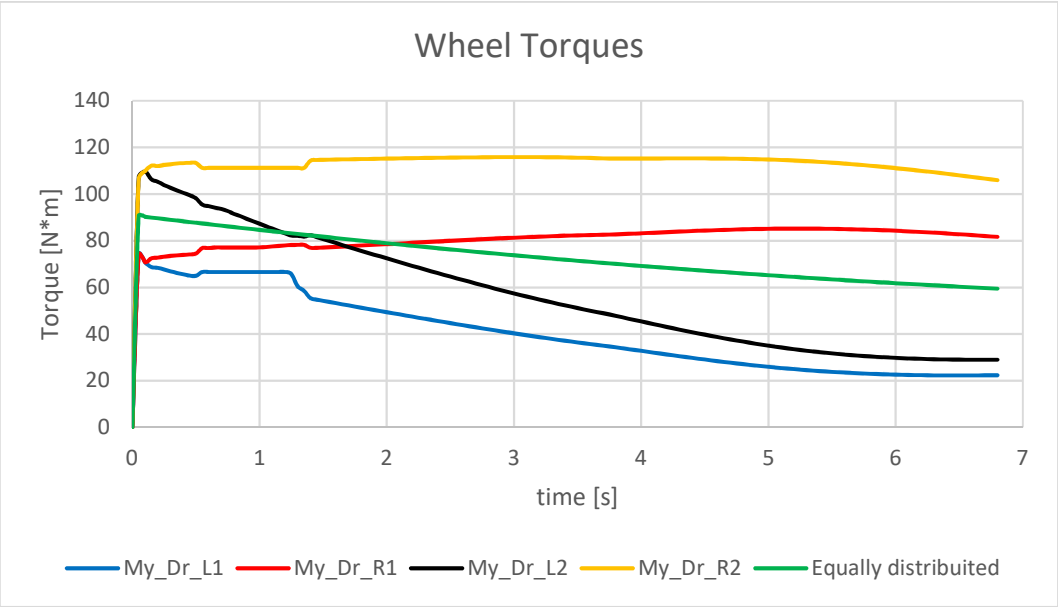

Figure 43: Wheel torques allocation for a constant steer input of 10°

One of the main advantages of using a TV control system is the ability to reach higher lateral acceleration with the same steer input. This can be also evaluated from the previous charts where the longitudinal speed of the vehicle is equal, but the cornering radius are not (remembering that the steer input is kept constant all over the simulation). In figure 45 it's represented the lateral acceleration of CG vs time for the chosen simulation.

The vehicle with TV reaches higher values of lateral acceleration; at the end of the simulations the vehicle with TV can reach a lateral acceleration equal to 1,4 g, instead the vehicle without TV reaches a value almost equal to 1,2 g.

It may seem strange that the vehicle can reach lateral acceleration higher than 1 g, since the adherence coefficient of the ground is set up equal to 1. This is due to the presence of aerodynamic components in the vehicle which, as the speed increases, guarantee a greater load on the wheels thus guaranteeing higher values of lateral and longitudinal acceleration comparing with considering only the weight loads on the wheels.

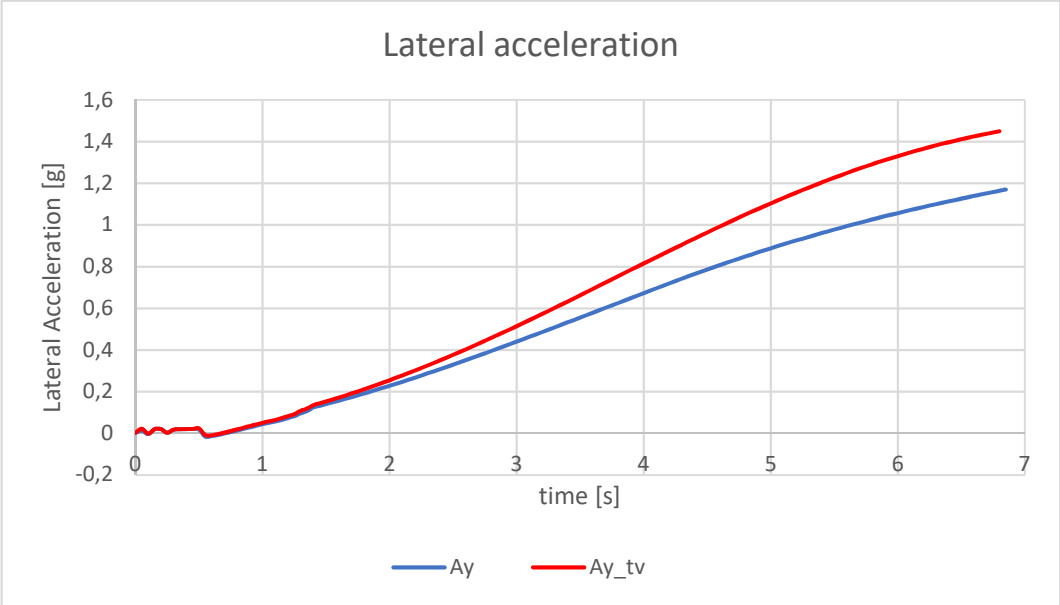

Figure 44: Lateral acceleration for a constant steer input of 10°

It can be seen in figure 45 how the vehicle with TV is able to perform an higher lateral acceleration all along the simulation.

One of the main parameters to evaluate the effectiveness of a torque vectoring controller is the acceleration gain that's represented in figure 46.

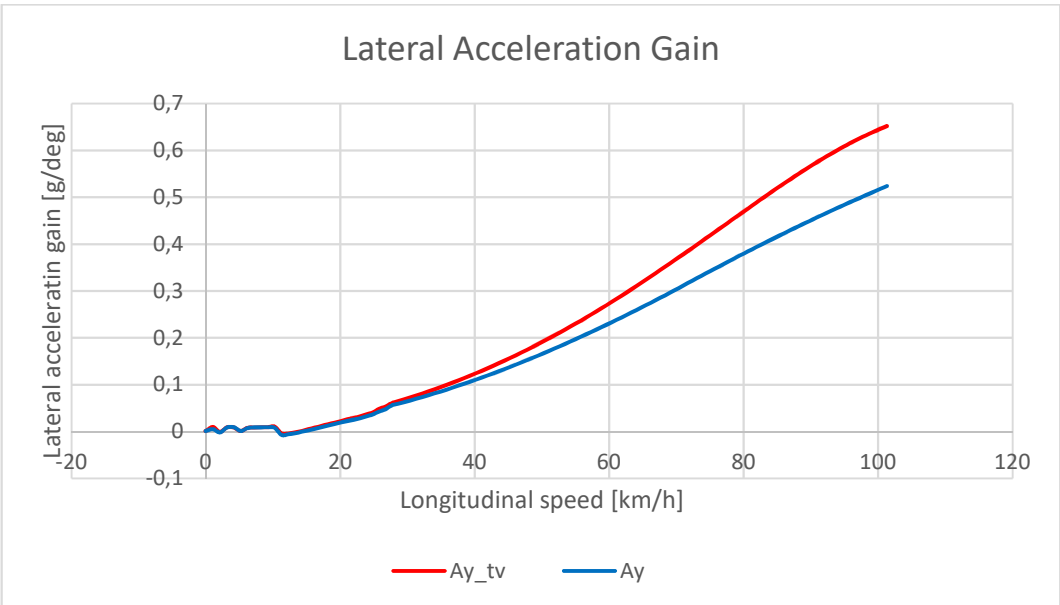

Figure 45: Lateral acceleration gain for a constant steer input 10°

Lateral acceleration gain is defined as the ratio between the lateral acceleration and the steering angle of the front wheels that can be easily calculated from the steer angle considering the fixed steer-wheel ratio S_r. As it's possible to see in figure 46,

the vehicle with TV reaches higher values of lateral acceleration gains for every value of the longitudinal speed of the vehicle, thus guaranteeing a better overall cornering behaviour. For the same steer input the vehicle with TV can then perform narrower radius turns without compromising the vehicle's longitudinal speed.

The yaw rate of the vehicle is represented in figure 47. The reference yaw rate value increases with time since the speed of the vehicle increase with time as stated in figure 43.

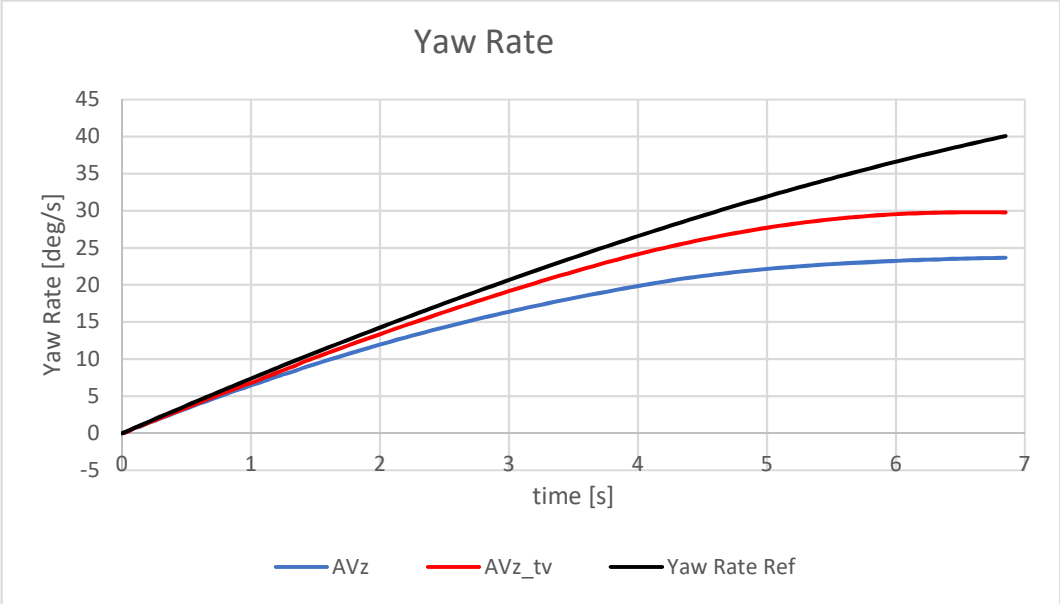

Figure 46: Yaw rate for a constant steer input 10°

The vehicle with TV can reach a yaw rate value nearer to the target reference one; both the vehicle with or without TV are not able to reach the reference value of yaw rate for high speed of the vehicle due to the fact that the vehicle is used at half of the maximum power (50% of the throttle is kept constant) so the effectiveness of the TV controller is limited.

In figure 48 it's represented the yaw rate gain in function of the velocity speed of the vehicle. As it was for lateral acceleration gain, yaw rate gain is defined as the ratio between yaw rate and steer angle of the front wheels; this parameter is also used to evaluate the effectiveness of TV.

As it's possible to see, ideally with the formula (61) used to calculate the yaw rate reference of the vehicle, it tends to be slightly oversteering (black curve).

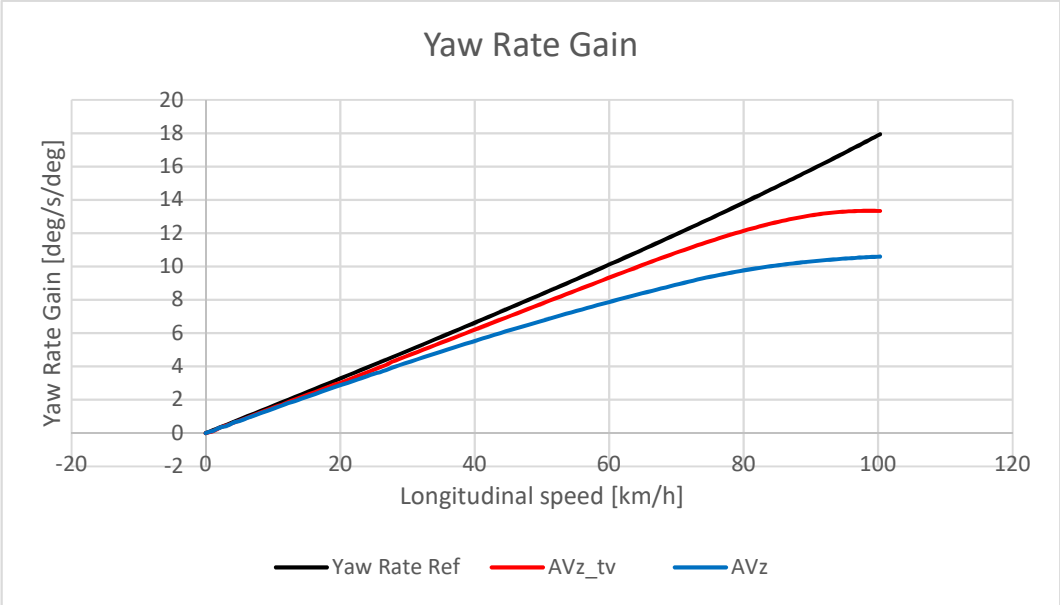

Figure 47: Yaw rate gain for a constant steer input of 10°

Both the vehicle with and without TV tend to have an understeer directional behaviour as it was stated before when considering figure 42. The vehicle with TV can reach higher values of yaw rate for the same steer input for each velocity speed of the vehicle; this guarantees a vehicle able to enter in curve faster and with better cornering performance. The application of TV guarantees reduction in the understeer behaviour of the vehicle.

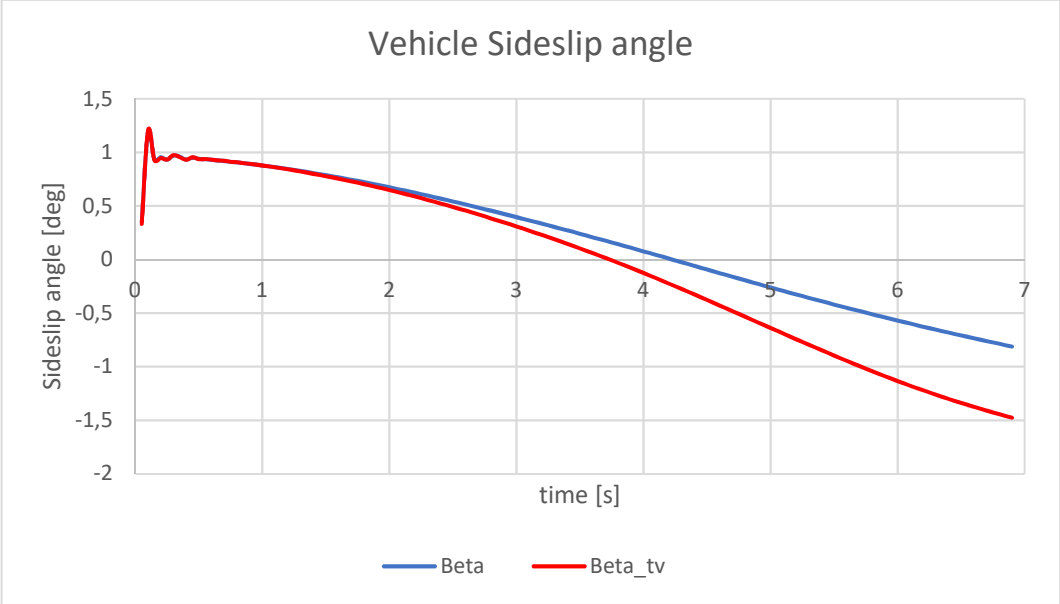

Figure 48: Vehicle side-slip angle for a constant steer input of 10°

Regarding stability, the parameter side-slip angle β should be minimized and its ideal value should be zero; but the TV control system designed uses a yaw rate reference tracking and does not command directly the parameter β. From figure 49 it's possible to see that the vehicle with TV reaches higher values of side-slip angle, but these values are still considerable small not adversely affecting the driving stability of the vehicle.

4.5.2 #2 Constant Steer Input of 20°

This simulation is performed with a constant steer input equal to 20 deg. The results of the simulations are presented and commented here below. The simulation ends when the vehicle reaches a value of longitudinal speed equal to 80 km/h.

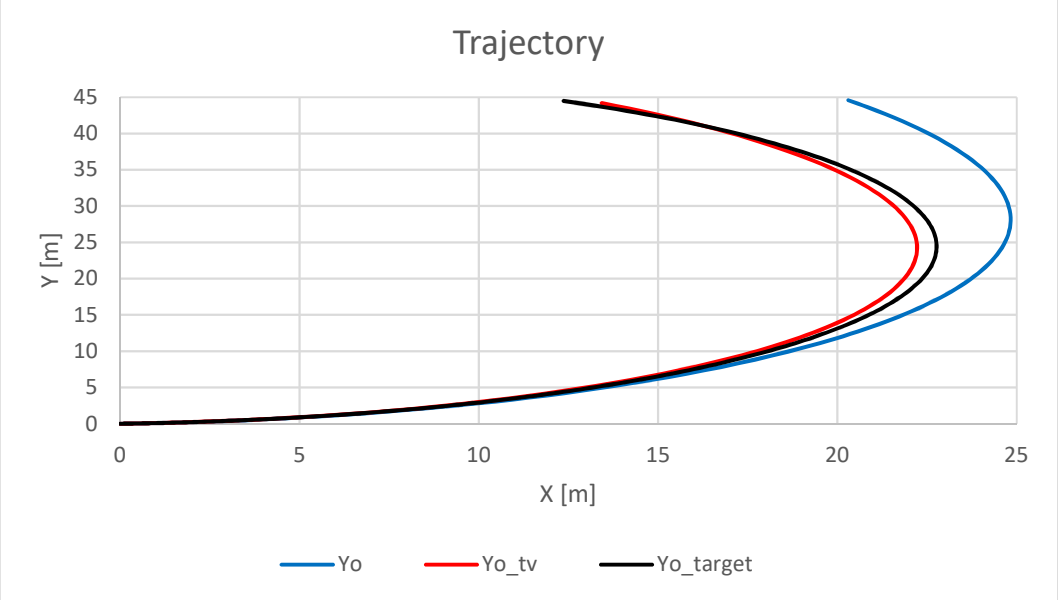

Figure 49: Plot of the vehicle trajectory for a constant steer input of 20°

In figure 50 the three paths of the vehicle are represented. The black curve represents the ideal vehicle path with the constant steer input of 20° performed at low velocity; the other two curves indicate the trajectory when using the TV

controller (red curve) and without the controller (blue curve). As it possible to see the vehicle with TV follows better the ideal curve. The vehicle without TV tends to move far away from the target curve; instead, due to the correct torque allocation among wheels, the vehicle with TV tends to be nearer to the target trajectory. The vehicle with TV seems to overcorrect the trajectory resulting in a curvature radius smaller than the target case.

As it was for the case with 10° steer input there's no main difference in the longitudinal speed between the two cases as it can be seen in figure 51.

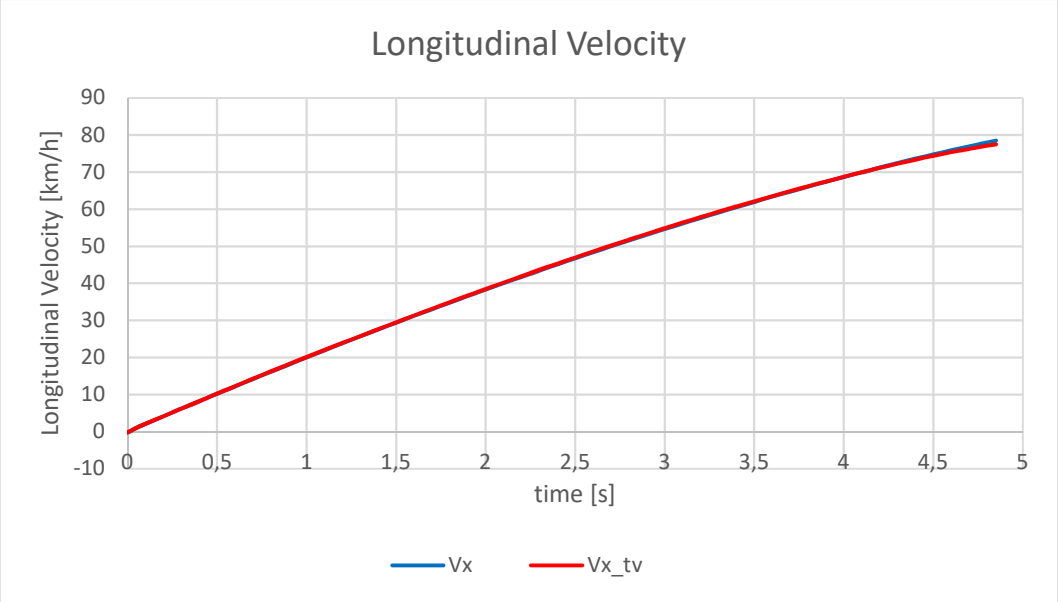

Figure 50: Plot of the vehicle longitudinal speed for a constant steer input of 20°

As it was previously done for the steer input of 10°, it's now calculated the amount of deviation of the trajectories with and without torque vectoring with respect to the ideal target trajectory. The values of RMSD and NRMSD are then calculated with the equations (77) and (78) and the results are reported in table 8.

DEVIATION TABLE	TV	NO TV
NRMS	**0,466**	**3,50**
NRMSD	**0,010**	**0,078**

Table 8: Normalized root mean square deviation for a constant steer input of 20°

The results obtained states that the vehicle with TV can follow the target trajectory in a better way obtaining a NRMSD value about 8 times smaller than the case without TV.

In figure 52 it's represented how the torque is allocated among the four wheels.

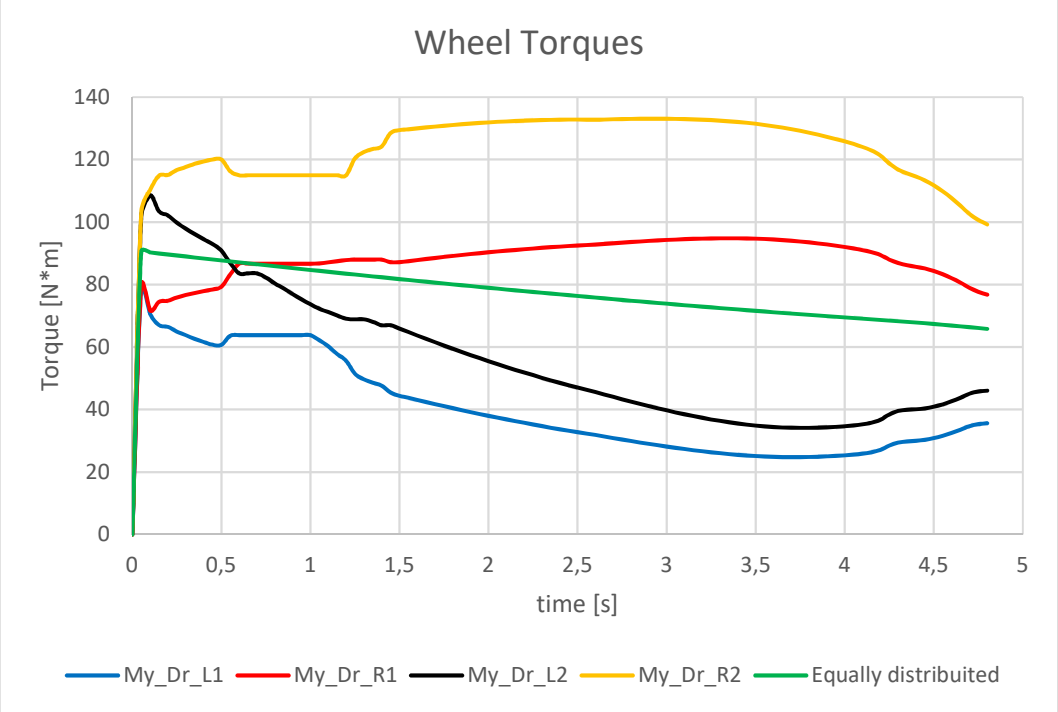

Figure 51: Wheel torques allocation for a constant steer input of 20°

It's possible to see how considering the same axle the external wheel (in this case the right one) has higher value of torque; this fact allows the vehicle to perform a curve with lower cornering radius with the same steer input, guaranteeing thus higher levels of lateral accelerations.

One of the main advantages of using a TV control system is the ability to reach higher values of lateral acceleration with the same steer input. This can be also evaluated from the previous charts where the longitudinal speed of the vehicle is equal, but the cornering radius are not. In figure 53 it's represented the lateral acceleration of CG vs time for the chosen simulation.

The vehicle with TV reaches higher values of lateral acceleration; at the end of the simulations the vehicle with TV can reach a lateral acceleration equal to about 1,6 g, instead the vehicle without TV reaches a value almost equal to 1,4 g. It's

good to be remembered that two cases have the same value of steer input from the driver.

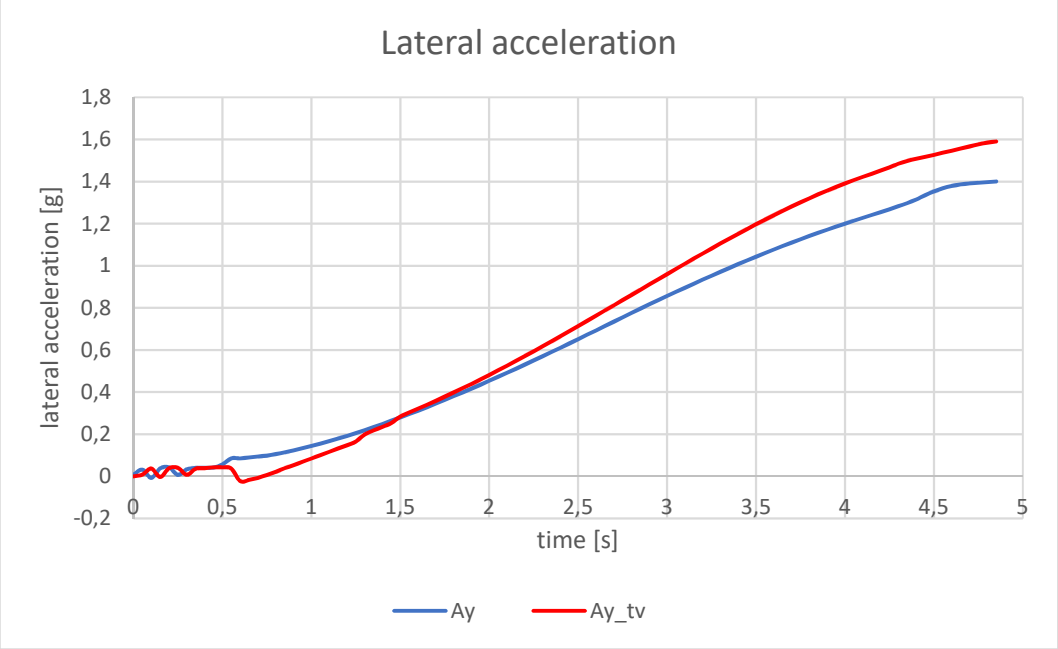

Figure 52: Lateral acceleration for a constant steer input of 20°

It may seem strange that the vehicle can reach lateral acceleration higher than 1 g, since the adherence coefficient of the ground is set up equal to 1. This is due to the presence of aerodynamic components in the vehicle which, as the speed increases, guarantee a greater vertical load on the wheels allowing the vehicle to reach higher accelerations.

In figure 53 it's possible to see how the vehicle without TV reaches higher values of lateral acceleration in the first seconds of the simulation and then the values are lower than the case with TV.

To evaluate the effectiveness of the controller it's used the parameter lateral acceleration gain represented in figure 54. Lateral acceleration gain is defined as the ratio between the lateral acceleration and the steering angle of the front wheels. As it's possible to see the vehicle with TV reaches higher values of lateral acceleration gains for speed higher than 30 km/h being able to assume higher values of lateral acceleration for the same value of steer input. So, the TV guarantees the vehicle to perform better in cornering condition.

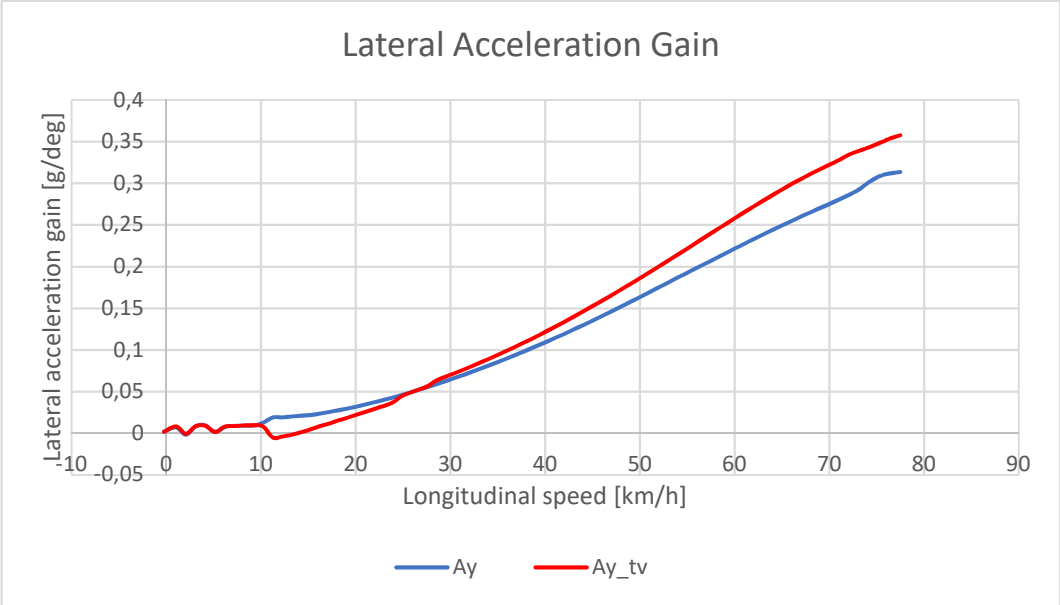

Figure 53: Lateral acceleration gain for a constant steer input 20°

The parameters yaw rate and its reference are represented in figure 55. It's possible to state that the vehicle with TV can perform better than the vehicle without TV reaching values of yaw rate closer to the reference ones. For high values of velocities, also the vehicle with TV can not reach the value of reference of yaw rate; this is mainly due to the real directional behaviour of the vehicle influenced by the presence of the anti-roll bar in the front axle that is not considered when computing the understeer gradient with the equation (56).

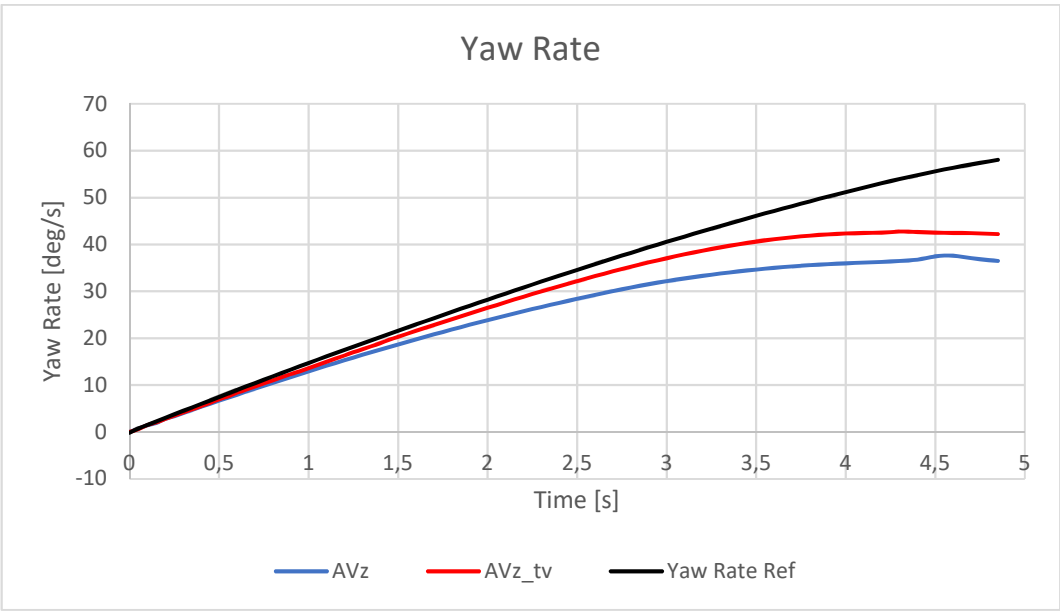

Figure 54: Yaw rate for a constant steer input 20°

In figure 56 it's represented the yaw rate gain in function of the velocity speed of the vehicle. As it's possible to see ideally with the formula (61) used to calculate the yaw rate reference of the vehicle the vehicle tends to be slightly oversteering; but it's possible to state that the real behaviour of the vehicle is understeering due to the presence of the anti-roll bar in the front axle of the vehicle. The application of TV changes the directional behaviour of the vehicle being less understeering as it's possible to see in figure 56.

The higher value of yaw rate gain guarantees the vehicle to perform better when cornering being able to enter in a faster way in the required turn.

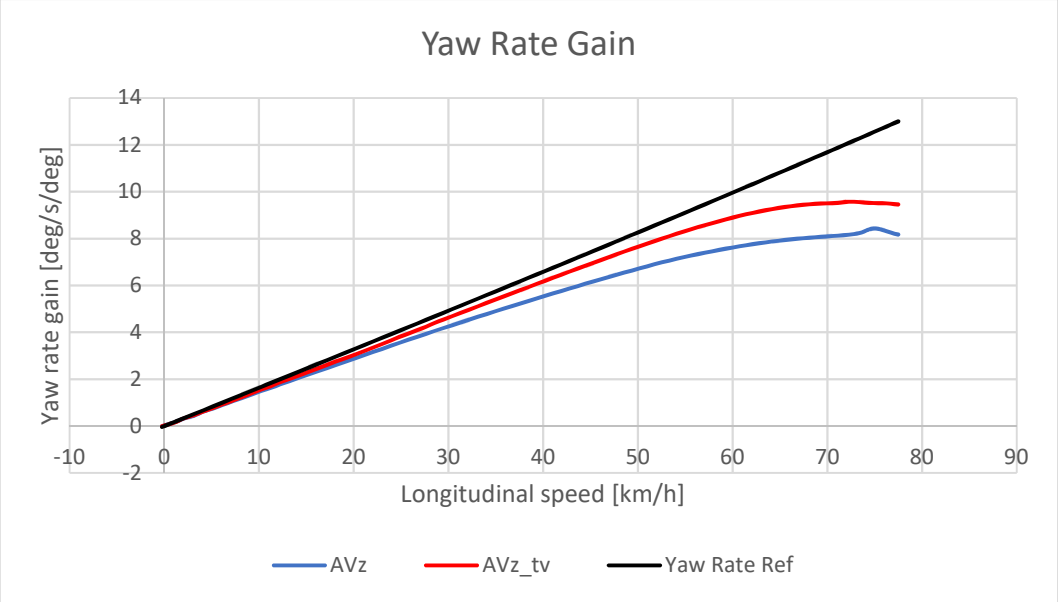

Figure 55: Yaw rate gain for a constant steer input of 20°

Regarding stability, the parameter side-slip angle β should be minimized and its ideal value should be zero. But the TV control system uses a yaw rate reference tracking and does not command directly the parameter β. From figure 57 it's possible to see that the vehicle with TV reaches higher values of side-slip angle, but these values are still considerable small not adversely affecting the driving stability of the vehicle.

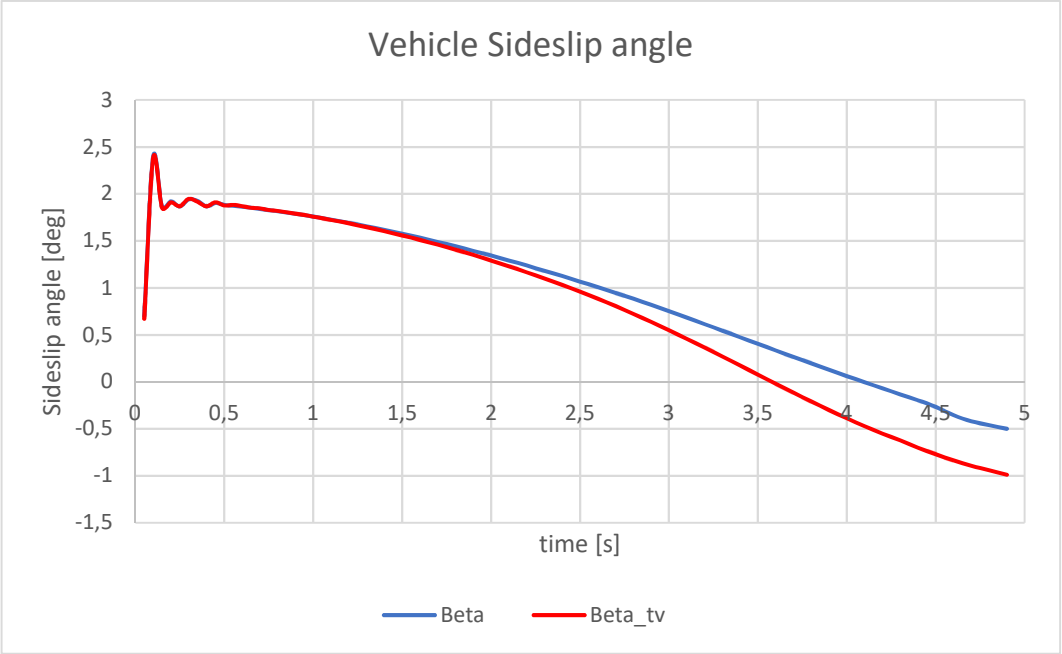

Figure 56: Vehicle side-slip angle for a constant steer input of 20°

4.6 Simulation: DOUBLE LANE CHANGE

The double lane change manoeuvre has been chosen for its complexity and to evaluate the overall handling of the vehicle. The manoeuvre was performed with an initial speed equal to zero and a full throttle requirement by the driver.

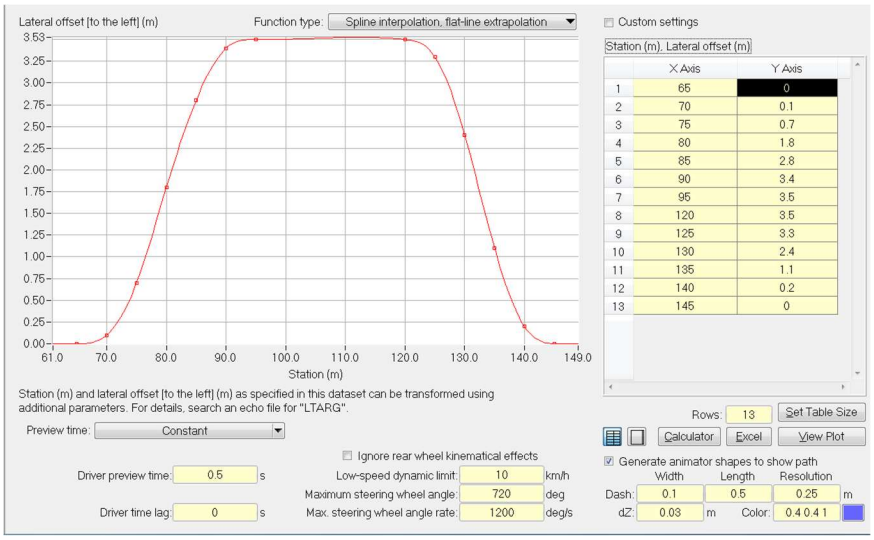

Figure 57: Target double lane change path

During the simulation the vehicle try to follow the ideal double lane change target; this simulation is done as closed-loop simulation since the vehicle has to follow a pre-defined trajectory. The ideal target trajectory is represented in figure 58. The manoeuvre is a double line change with a lateral offset of about 3,5 metres.

Two simulations are carried on, with and without the TV system to test its effectiveness. In figure 59 it's represented the trajectory result of the simulations.

It can be seen how the vehicle with TV perform a trajectory that is closer to the target one as it was for the two constant steer simulation already discussed.

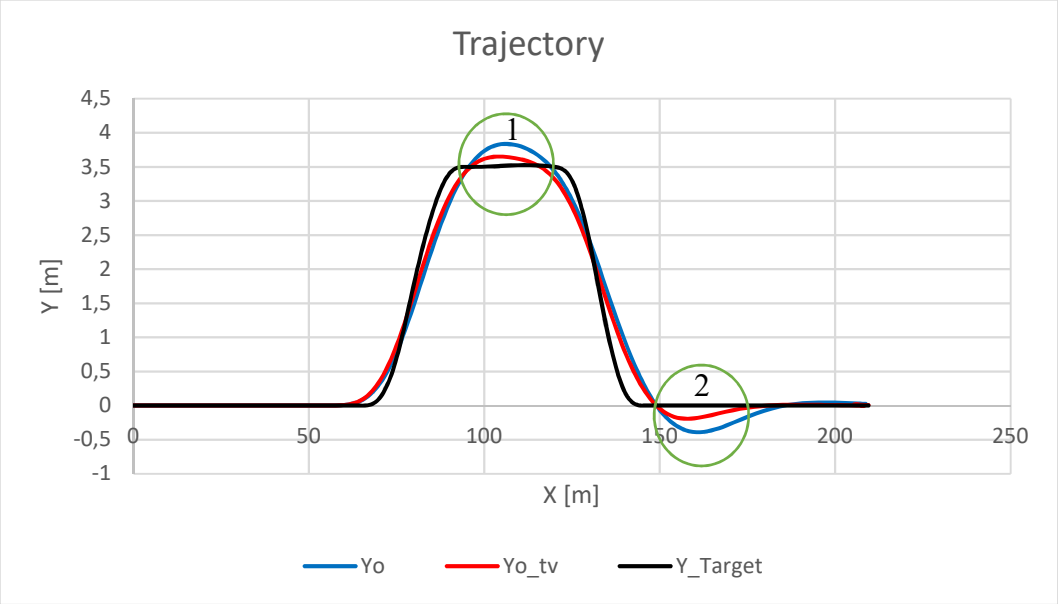

Figure 58: Path of the vehicle for double lane change manoeuvre

The maximum offset of the two trajectories with respect to the target one can be computed in the two points represented with green circles in figure 59. The results are reported in table 9.

MAXIMUM OFFSET	WITHOUT TV	WITH TV
1	**0,31 m**	**0,11 m**
2	**-0.39**	**-0,19 m**

Table 9: Offset from the target curve for the double lane change manoeuvre

It can be seen how the vehicle with TV is able to reach maximum offset values smaller than the case without TV. It can also be stated, from figure 59, that the vehicle without TV needs more time to stabilize at the end of the final curve.

Using the formulas (77) and (78) it's possible to calculate the amount of deviation from the target trajectory and the results are presented in the table 10.

DEVIATION TABLE	TV	NO TV
NRMS	0,225	0,288
NRMSD	0,064	0,082

Table 10: Normalized root mean square for double lane change manoeuvre

The values obtained states how the vehicle with TV can follow better the target curve; however, the results obtained are not as strong as those obtained in the two cases of constant steer input manoeuvres. In fact, the vehicle without TV has NRMSD value only 1,3 higher than the case with TV.

The vehicle without TV tends to overshoot in both turns; the vehicle with TV instead tends to follow the trajectory faster guaranteeing a better cornering performance of the vehicle.

The longitudinal speed of the vehicle for both the simulations (represented in figure 60), with or without TV has mainly no difference with the vehicle with TV that at the end of the simulation reaches a slightly higher value of longitudinal speed when finishing the manoeuvre.

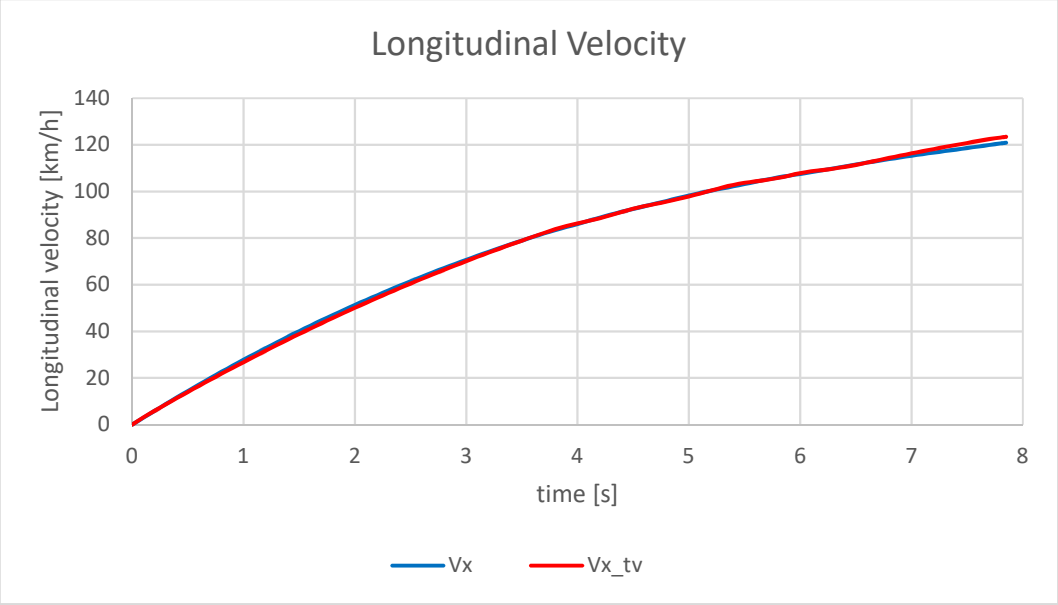

Figure 59: Longitudinal speed for the double lane change manoeuvre

The lateral acceleration of the vehicle is represented in figure 61 and the two curves are similar; the main differences are stated here below:

- The vehicle with TV reaches an absolute value of lateral acceleration smaller when reaching the pick of the trajectory
- The lateral acceleration curve with TV is out of phase with respect to the other curve in the final turn

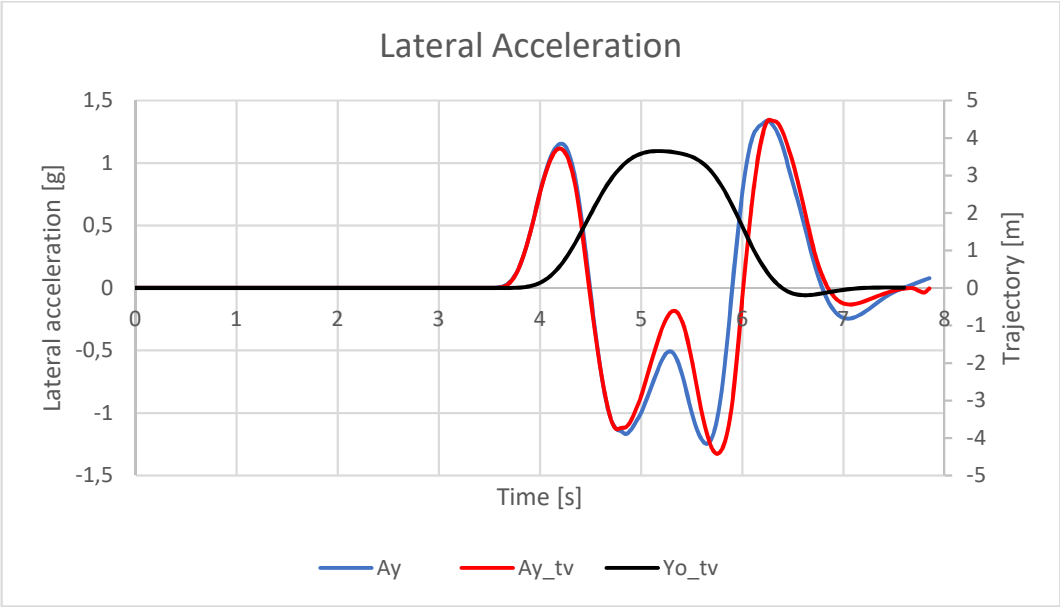

Figure 60: Lateral acceleration for the double lane change manoeuvre

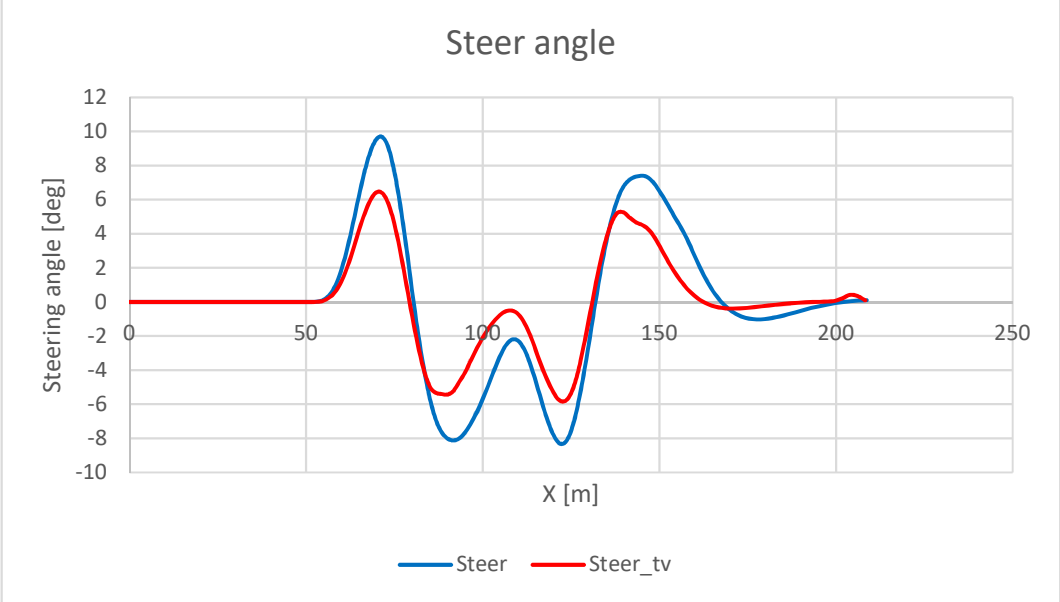

Figure 61: Steer input for double lane change manoeuvre

Since the lateral acceleration of the vehicle is almost similar in both cases, to evaluate properly the effectiveness of the controller it's decided to use the steer input represented in figure 62, remembering that the acceleration gain previously defined is the ratio in between the lateral acceleration and the steering angle of the front wheels.

As it's possible to see in figure 62, the vehicle with TV guarantees to complete the simulation with lower angle of the steer; this means that the vehicle's cornering behaviour has been improved all over the manoeuvre.

In figure 63 it's represented the wheel torque allocation and the trajectory of the vehicle with TV. As it's possible to see the torque varies a lot when performing the lane change. For the first part where the curve is performed to the left a higher amount of torque is given to the right wheels; when the vehicle reaches the changes line, the torque is increased to the left wheels and decreased to the right one to avoid overshoot of the trajectory. Then, at the end for the right turn, the torque is increased to the left wheels and when the lane change is performed the torque is increased to the right wheels and decreased to the left ones to guarantee a faster stabilization of the vehicle at the end of the manoeuvre.

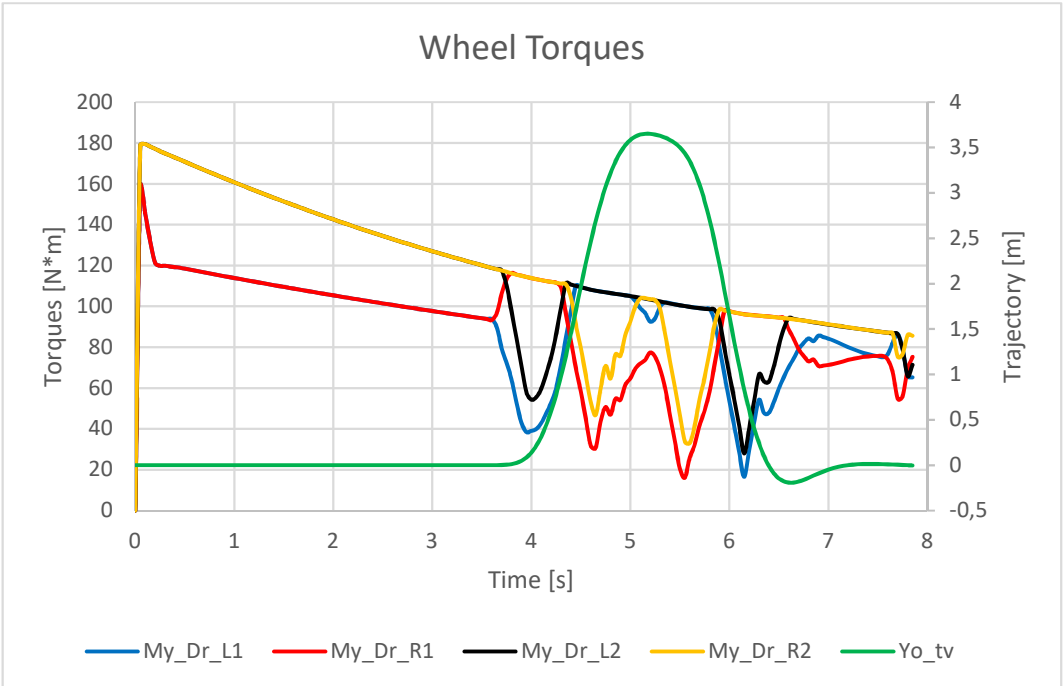

Figure 62: Wheel torques allocation for double lane change

In figure 64 it's represented the yaw rate for the simulation carried on. It's possible to state that the vehicle with TV can better follow the ideal yaw reference calculated with the equation (61).

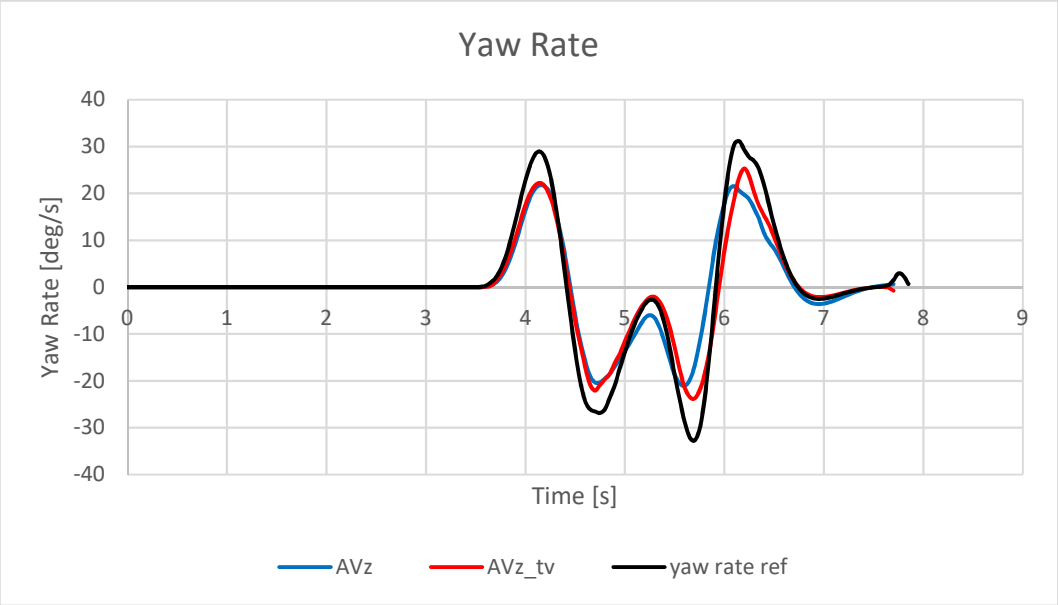

Figure 63: Yaw rate for double lane change manoeuvre

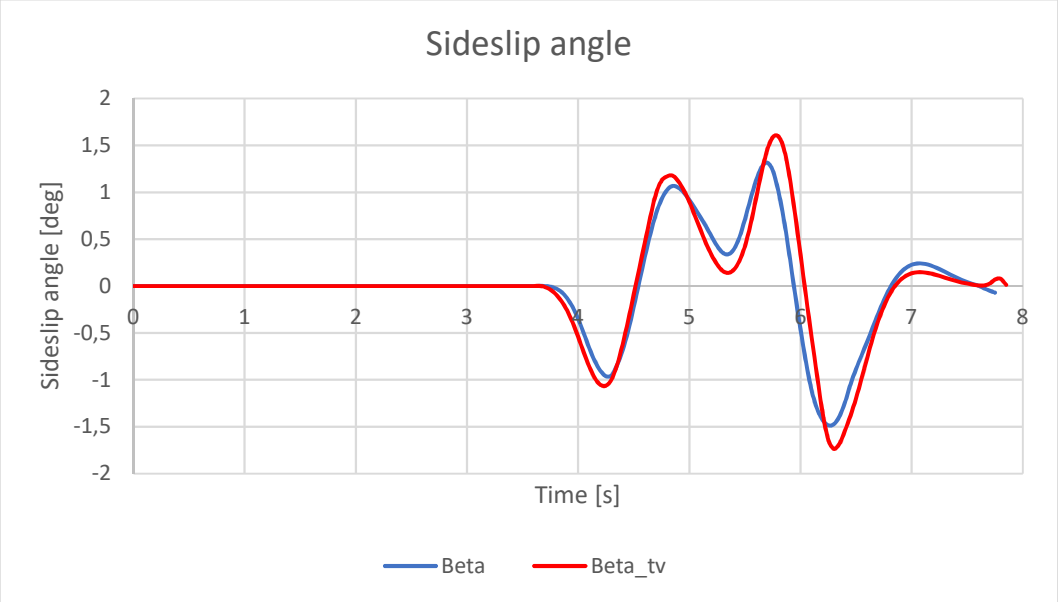

Figure 64: Side-slip angle for the double lane change manoeuvre

In figure 65 it's represented the side-slip angle of the vehicle. As it's possible to see the vehicle with TV reaches slightly higher values of side-slip angle than the case

without TV, but still these values are considerable small and do not affect the stability behaviour of the vehicle.

Conclusions and future work

In this work a dynamic control system has been proposed for an in-wheel electric vehicle participating at the Formula SAE engineering competition. The presented Torque Vectoring (TV) system is based on yaw rate ($\dot{\psi}$) system tracking in order to enhance the vehicle dynamics in various manoeuvres.

The proposed control system considers both lateral and longitudinal torque distribution based on the vertical load on the wheels and on the required z-axis moment to improve the vehicle's trajectory. The system can minimize wheel slip enhancing the cornering dynamic behaviour of the vehicle in different manoeuvres. On the other side, TV was also able to increase the stability of the vehicle also in the double lane change manoeuvre guaranteeing a better tracking of the target trajectory, which is the most important aspect of this manoeuvre. Additionally, the proposed dynamic control system results in an understeering behaviour reduction in all the presented simulations.

At the end, this control system has been able to better follow the yaw rate reference and the target trajectory, proving a real cornering enhancement due to the correct torque distribution among wheels.

Future work will include factors that have not been considered in the proposed Simulink model such as:

- Complex tire model
- Lateral load distribution due to the anti-roll bar
- More complex vehicle model then the used 2 DOF Bicycle model, in order to consider not only flat motion of the car
- Study of the steering geometry, not considering a fixed ratio between steer and front wheels.
- Real road testing to analyse the veracity of the results

One of the main disadvantages of the in-wheel motors configuration proposed by the studied vehicle is the big increase in weight of the unsprung mass. This leads to

a different dynamic behaviour of the vehicle and more tire wears. One future solution could be mounting the four electric motors inside the body in white of the vehicle that guarantees the independent allocation of torque without increasing the unsprung mass of the vehicle

Bibliography

[1] Site: https://amk-group.com/en/product/amk_servomotors

[2] Site: https://en.wikipedia.org/wiki/Inertial_frame_of_reference

[3] William F. Milliken, Douglas L. Milliken [Race_Car_Vehicle_Dynamics]

[4] Site: http://www.mechademic.com/courses/course_detail/21/

[5] Site: https://www.researchgate.net/figure/Tire-Axis-Terminology_fig1_264991925

[6] Site: https://www.hoosiertire.com/

[7] Massimo Giuggiani [The Science of Vehicle Dynamics: Handling, Braking, and Ride of Road and Race Cars]

[8] Massimo Giuggiani [Dinamica del veicolo]

[9] Giancarlo Genta [Meccanica dell'autoveicolo]

[10] Alberto Parra, Asier Zubizarreta, Joshue Perez, Martin Dendaluce [Intelligent Torque Vectoring Approach for Electric Vehicles with Per-Wheel Motors]. Research Article 2018

[11] Chengning Zhang, Yu Zhao, Yong Chen [An Electric Stability Control System to Improve Stability for an Eight In-wheel Motor Independent Drive Electric Vehicle]. Research Article 2017

[12] Li Zhai, Rufei Hou, Steven Kavuma [Continous Steering Stability Control of a Four In-Wheel Motor Drive Electric Vehicle on a Road with Varying Adhesion Coefficient]. Research Article 2017

[13] João Pedro Marques Antunes [Torque Vectoring for a Formula Student Prototype]. Master Thesis

[14] Shayan Taherian [Integrated control of Four-Wheel-Steering and Torque vectoring]. Master Thesis

[15] Martin Mondek [Active torque vectoring systems for electric drive vehicles]. Master Thesis

[16] Gerd Kaiser [Linear Parameter-Varying Control for an Electric Vehicle]. Master Thesis

[17] Anton Stoop [Design and Implementation of Torque Vectoring for the Forze Racing Car]. Master Thesis

[18] Almeida Vianna [Torque Vectoring in Electric Vehicles with In-wheel Motors]. Master Thesis